Research Square

Preprints are preliminary reports that have not undergone peer review.
They should not be considered conclusive, used to inform clinical practice,
or referenced by the media as validated information.

Genome-wide identification of the SAUR gene family and screening for SmSAURs involved in root development in Salvia miltiorrhiza

Wei Wang
Yangzhou University
Yuwei Zheng
Yangzhou University
Lin Qiu
Yangzhou University
Dongfeng Yang
Zhejiang Sci-Tech University
Ziyang Zhao
Yangzhou University
Yuanyuan Gao
Yangzhou University
Ru Meng
Yangzhou University
Hongguang Zhao
Shaanxi Tasly Plants Pharmaceutical Co., Ltd
Shuncang Zhang
zhangsc@yzu.edu.cn

Yangzhou University https://orcid.org/0000-0001-6856-0408

Research Article

Keywords: Salvia miltiorrhiza, Root development, Small auxin-up RNA, Transcriptome, Pearson correlation coefficient

Posted Date: February 20th, 2024

DOI: https://doi.org/10.21203/rs.3.rs-3931460/v1

License: This work is licensed under a Creative Commons Attribution 4.0 International License. Read Full License

Version of Record: A version of this preprint was published at Plant Cell Reports on June 11th, 2024. See the published version at https://doi.org/10.1007/s00299-024-03260-5.

Abstract

Salvia miltiorrhiza is a widely utilized medicinal plant in China. Its roots and rhizomes are the main medicinal parts and crucial in determining the quality of the herb. Previous studies reveal that auxin plays pivotal roles in S. miltiorrhiza root development. As the crucial early auxin-response genes, whether small auxin-up RNA genes (SAURs) are involved in the auxin-mediated root development in S. miltiorrhiza is worthy of investigation. In this study, 55 SmSAUR genes in S. miltiorrhiza were identified and their physical and chemical properties, gene structure, cis-acting elements, and evolutionary relationship were analyzed. The expression levels of SmSAUR genes in different organs of S. miltiorrhiza were detected by RNA-seq combined with qRT-PCR. The root development of S. miltiorrhiza seedlings was altered by the application of indole-3-acetic acid (IAA) and Pearson correlation coefficient analysis was conducted to screen SmSAURs that potentially participate in this physiological process. As the results shown, the diameter of primary lateral root was positively correlated with SmSAUR4. The secondary later root number was positively correlated with SmSAUR18 and negatively correlated with SmSAUR4. The root length showed a positive correlation with SmSAUR28 and SmSAUR37 and a negative correlation with SmSAUR38. The root fresh biomass exhibited a positive correlation with SmSAUR38 and a negative correlation with SmSAUR28. The SmSAURs mentioned above were probably involved in the auxin-mediated root development in S. miltiorrhiza. Our study presents a comprehensive overview of SmSAURs and establishes the groundwork for elucidating the molecular mechanism underlying root morphogenesis in this species.

Key Message

***SmSAUR*4, *SmSAUR18*, *SmSAUR28*, *SmSAUR37*, and *SmSAUR38* were probably involved in the auxin-mediated root development in *Salvia miltiorrhiza*.**

Introduction

Salvia miltiorrhiza is a widely recognized traditional Chinese medicine (TCM) in China. Its main bioactive compounds are hydrophilic phenolic acids and lipophilic tanshinones (Ren, et al. 2019; Wu, et al. 2020). This herb is commonly utilized in the treatment of cardiovascular diseases (Ren, et al. 2019; Wang, et al. 2017), hepatocirrhosis (Lin, et al. 2006), and menstrual alleviation (Lee, et al. 2020). The primary medicinal parts of *S. miltiorrhiza* are roots and rhizomes, and the morphology of the roots plays a vital role in determining the yield and quality of this herb (Xie, et al. 2023). However, the molecular mechanisms regulating root development of *S. miltiorrhiza* have not yet been completely elucidated. Previous studies have demonstrated that auxin, a decisive hormone, is involved in regulating root development in *S. miltiorrhiza*. For instance, Zhang et al. (2023) demonstrate that applying 10 μmol·L^{-1} indole-3-acetic acid (IAA) promotes root development in *S. miltiorrhiza*, while 20 μmol·L^{-1} N-1-naphthylphthalamic acid (NPA) inhibits this biological proces. Exogenous IAA decrease the expression level of the root growth inhibitor *SmMYB52*, thereby indirectly influencing the root biomass and root length of *S. miltiorrhiza* (Wang, et al. 2021). Cao et al. (2021) find that treatment with 100 μmol·L^{-1} IAA significantly suppresses the expression level of *SmSPL6*, a promoter of root elongation in *S. miltiorrhiza*. In conclusion, auxin is an indispensable factor that affects root devolopment in *S. miltiorrhiza*, and its precise regulatory mechanism requires to be further studied.

SAUR is a considerable gene family exclusively found in plants and is sensitively responsive to auxin (Stortenbeker and Bemer 2019). The *SAUR* gene family plays an essential role in regulating plant root development (Chen, et al. 2014). In *A. thaliana*, *AtSAUR41* promotes auxin transport in the hypocotyl, regulates hypocotyl elongation and increases the number of lateral roots. Driven by the *AtPIN2* and *AtPLT2* promoters, *AtSAUR41* enhance root geotropism (Kong, et al. 2013). Overexpression of *CsSAUR31* in cucumber promotes root and hypocotyl elongation (Luan, et al. 2023). *OsSAUR45* inhibits the expression of *OsYUCCA* and *OsPIN*, which affects the synthesis and transport of auxin and leads to a reduction in adventitious roots and shortening of primary roots in *Oryza sativa* (Xu, et al. 2017). *TaSAUR75* overexpression *Triticum aestivum* lines show longer root morphology in response to drought and salt stress (Guo, et al. 2018). Nevertheless, the specific regulatory mechanisms of the *SAUR* gene family in the root development remains to be further studied in *S. miltiorrhiza*. SAUR proteins are small proteins with a molecular weight ranging from 9 to 30 kDa that can be rapidly synthesized after exposure to auxin. The central region of the SAUR protein typically contains a highly conserved domain consisting of approximately 60 amino acids, while the C-terminus and N-terminus show relatively less conservation (Hu, et al. 2018; Ren and Gray 2015). However, due to functional redundancy and instability, there are relatively few studies on *SAUR* genes. Single knock-outs of *SAUR* genes seldom produce mutant phenotypes due to functional redundancy (Sun, et al. 2016; van Mourik, et al. 2017). Approximately 70% of *SAUR* genes respond to auxin in *Arabidopsis thaliana*, but some are not regulated by auxin (van Mourik, et al. 2017).

In this study, we identified and comprehensively analyzed the *SmSAUR* gene family in *S. miltiorrhiza*. We investigated their physical and chemical properties, chromosomal distribution, phylogenetic relationships, *cis*-acting elements, gene structure, motifs, conserved domains, as well as expression profiles in different organs. Subsequently, the root development of *S. miltiorrhiza* was altered by the application of IAA and Pearson correlation coefficient analysis was employed to sceen *SmSAUR* genes that potentially contribute to the root development in *S. miltiorrhiza*. Our study expands the understanding of the characteristics of *SmSAUR* gene family in *S. miltiorrhiza* and provides valuable insights into revealing the roles of *SmSAUR* genes in regulating the auxin-mediated root development in this medicinal plant.

Materials and methods

Plant materials and treatments

Total RNA was extracted from the roots, stems, leaves, and flowers of one-year-old *S. miltiorrhiza* collected from the plantation base of Yangzhou University (32° 23' 49.99" N, 119° 26' 8.99" E). Seed germination followed the method used in previous study by Zhang et al. (2023). At the first true leaf stage, seedlings with the same growth status were selected for further investigations. Two treatment groups were set up in this study, including 0.10

μmol·L^{-1} IAA-treated and control groups. The selected seedlings were randomly divided into two groups, each consisting of twelve biological replicates. The experimental seedlings were grown hydroponically using Hoagland solution (HPHS) (Zhu, et al. 2023), with nutrient composition based on the Hoagland solution supplemented with weakly acidic and ammonia sources. The storage solution was stored at 4°C. Then, the storage solution was diluted 20-fold before being used and its pH was adjusted to between 5.8 and 6.5 using 1 mol·L^{-1} NaOH solution. The nutrient solution for hydroponic seedlings was replaced every 3 days. After 2 months of treatment, the morphological indexes of the samples were determined, and the roots were collected for total RNA extraction.

Identification of the SAUR gene family in S. miltiorrhiza

The gene sequences of 79 *A. thaliana SAUR* genes (81 *AtSAUR* genes, including two pseudogenes) were obtained from the *A. thaliana* database TAIR (http://www.Arabidopsis.org/), and 58 *O. sativa SAUR* gene sequences were obtained from the National Data Center for Genome Sciences (https://ngdc.cncb.ac.cn/) (Jain, et al. 2006). Nucleotide Blast was used with a cutoff of E-value < 1×10^{-5} as the query sequence to search for the *SmSAUR* genes in *S. miltiorrhiza* genome databases (Altschul, et al. 1997). This *S. miltiorrhiza* genome databases were obtained from the GWH database (https://ngdc.cncb.ac.cn/gwh/Assembly/64073/show) (Pan, et al. 2023) of the China National Center for Bioinformation (https://ngdc.cncb.ac.cn/) (Lu, et al. 2020). The methods of gene identification were referenced in the previous study (Li, et al. 2022). Briefly, the Hidden Markov Model (HMM) profiles of the SAUR domain (PF02519) were obtained from the Pfam database (https://www.ebi.ac.uk/interpro/entry/pfam/) (Anai, et al. 1998), and the conserved domain of candidate *SmSAURs* was confirmed using the NCBI database (https://www.ncbi.nlm.nih.gov/cdd/) (Wang, et al. 2023). The theoretical isoelectric point (pI) and molecular weight (MW) of SmSAURs were analyzed using the Expasy online website (https://web.expasy.org/compute_pi/) (Gasteiger, et al. 2005; Wilkins, et al. 1999). The subcellular localization of SmSAUR proteins was predicted using the BUSCA online website (http://busca.biocomp.unibo.it/) (Savojardo, et al. 2018).

Phylogenetic analysis, chromosomal localization and synteny analysis

The construction of the phylogenetic tree referred to the previous method (Xu, et al. 2016), and ChiPlot (https://www.chiplot.online/tvbot.html) was used to enhance the visual appearance of the constructed phylogenetic tree (Xie, et al. 2023). The chromosomal localization and synteny analysis of *SmSAURs* were analyzed by the TBtools software (Chen, et al. 2023).

Gene structure and cis-acting elements analysis

SmSAUR proteins amino acid sequences were screened from the GWH database (https://ngdc.cncb.ac.cn/gwh/Assembly/64073/show). The motifs of SmSAUR proteins were analyzed using the MEME online website (https://meme-suite.org/meme/tools/meme) (Bailey, et al. 2009), with 10 motifs identified. The cis-acting elements were predicted and analyzed using the PlantCARE online tool (https://bioinformatics.psb.ugent.be/webtools/plantcare/html/) following the method previously described by Wang et al. (2021). The gene structure and distribution of *cis*-acting elements in the promoters were visualized using the GSDS online website (http://gsds.gao-lab.org/) (Hu, et al. 2014).

RNA-seq analysis

Samples of roots, stems, leaves, and flowers were collected from one-year-old *S. miltiorrhiza* seedlings for RNA-seq analysis, aiming to study gene expression profiles across different organs. The root samples from the IAA-treated and control groups were also collected for RNA-seq analysis to screen relevant functional gene. Transcriptome sequencing and analysis of the aforementioned sample batches were conducted by Majorbio company (Shanghai, China) and visualized using the Majorbio Cloud bioinformatics platform (https://cloud.majorbio.com/page/tools/) (Ren, et al. 2022). Differential expression of *SmSAURs* in diverse organs and treated groups was analyzed using the DESeq2 R package (1.10.1) (Love, et al. 2014), considering gene with $|\log_2^{(\text{Fold change})}| \geq 1$ and the adjusted *P* value < 0.05, as differentially expressed.

To further verify the relationship between *SmSAURs* and root development in *S. miltiorrhiza*, we conducted a correlation analysis between the expression levels of *SmSAURs* and root morphological indexes of the IAA-treated and control groups. This analysis utilized the Pearson correlation coefficient method as described by Xiao, et al. (2023). The correlation between the calculated values was denoted by r, with a positive value indicating a positive correlation and a negative value indicating a negative correlation. The absolute value of r reflected the strength of the correlation between the two variables. In general, if | r | < 0.40, it suggests that the two variables have no significant correlation. When | r | ≥ 0.60 and the adjusted *P* value < 0.05, both variables are considered significantly correlated.

RNA extraction, cDNA synthesis, and quantitative real-time (qRT)-PCR analysis

Total RNA samples from different organs, as well as the IAA-treated and control groups, were extracted and reverse transcribed into cDNA using the Vazyme Biotech (Nanjing, China) company's method (Wang, et al. 2022; Yu, et al. 2022). The genes expression levels were monitored using quantitative real-time PCR (qRT-PCR), following the methodology described in a previous study (Lu, et al. 2020). The relative expression levels of *SmSAURs* were calculated by the $2^{-\Delta\Delta Ct}$ method (Livak and Schmittgen 2001), with *SmActin* as the internal reference gene. Gene-specific primers were designed using CE Design v1.04 software and checked for specificity using SnapGene v4.1.9 software. Each sample hand three biological replicates (Bennett, et al. 2015).

Statistical analysis

Statistical analyses were performed to analyze gene expression and root phenotypes using IBM SPSS Statistics v26.0 software. The determination of statistically significant differences involved one-way analysis of variance (ANOVA) followed by Duncan's multiple range test ($P < 0.05$), one-way analysis of variance (ANOVA) followed by Fisher's least significant difference (LSD) test ($P < 0.05$), or two-tailed Student's t-tests ($P < 0.01$). IBM SPSS Statistics v26.0

was also utilized to analyze the correlation between the expression levels of *SmSAUR* genes and the root morphological indexes of *S. miltiorrhiza* under IAA treatment. The strength of the statistical correlation was assessed through bivariate correlation analysis, and for comparative purposes, followed by two-tailed Student's t-tests ($P < 0.01$).

Results

Genome-wide identification and chromosomal distribution of SAUR genes in S. miltiorrhiza

A total of 55 *SmSAUR* gene members were identified and named *SmSAUR1-SmSAUR55* according to their chromosomal location (Table 1, Table S1-S2). Focused subsequent analysis examined the physical and chemical properties of the identified *SmSAUR* genes. The cDNA length of *SmSAURs* varied from 243 bp (*SmSAUR1* and *SmSAUR45*) to 528 bp (*SmSAUR7*). The predicted MW of the SmSAUR proteins ranged from 9,126.74 Da (SmSAUR1) to 19,784.58 Da (SmSAUR7), while their theoretical pI ranged from 4.99 (SmSAUR5) to 11.07 (SmSAUR38). Subcellular localization analysis showed that 19 SmSAUR proteins were located in the nuclear, 24 SmSAUR proteins were predicted to be in the chloroplast, 11 SmSAUR proteins were located in the mitochondrion, and SmSAUR54 was located in the extracellular space. The results of protein hydrophilicity prediction indicated that only two SmSAUR proteins (SmSAUR11 and SmSAUR53) were hydrophobic, while the remaining members were hydrophilic proteins.

Table 1
Characteristics of *SmSAUR* genes and SmSAUR proteins in *Salvia miltiorrhiza*.

Gene name	Gene ID	Chromosome	Locus	CDS Length (bp)	Number of aa	Theoretical pI	Mw (Da)	Subcellular localization	Gravy
SmSAUR1	evm.model.HICASM0.1861	Chr 1	28402568–28402810	243	80	9.45	9126.74	chloroplast	-0.227
SmSAUR2	evm.model.HICASM0.2320	Chr 1	32715887–32716110	324	107	8.88	12004.97	nucleus	-0.155
SmSAUR3	evm.model.HICASM0.3206	Chr 1	41999990–42000415	426	141	10.68	15898.87	chloroplast	-0.204
SmSAUR4	evm.model.HICASM0.3700	Chr 1	47668156–47668614	459	152	5.26	17168.34	chloroplast	-0.633
SmSAUR5	evm.model.HICASM0.3702	Chr 1	47696575–47696949	375	124	4.99	13711.53	nucleus	-0.236
SmSAUR6	evm.model.HICASM0.3777	Chr 1	48614123–48614611	489	162	5.92	17997.4	mitochondrion	-0.131
SmSAUR7	evm.model.HICASM0.3856	Chr 1	49382273–49382800	528	175	8.86	19784.58	chloroplast	-0.505
SmSAUR8	evm.model.HICASM0.6011	Chr 1	69646200–69646709	510	169	9.77	19406.3	chloroplast	-0.447
SmSAUR9	evm.model.HICASM0.6012	Chr 1	69649056–69649349	294	97	9.36	11112.73	chloroplast	-0.319
SmSAUR10	evm.model.HICASM0.6013	Chr 1	69652982–69653311	330	109	9.61	12446.1	mitochondrion	-0.398
SmSAUR11	evm.model.HICASM0.6015	Chr 1	69666294–69666623	330	109	8.49	12136.98	chloroplast	0.04
SmSAUR12	evm.model.HICASM0.6016	Chr 1	69669389–69669700	312	103	7	11776.54	chloroplast	-0.277
SmSAUR13	evm.model.HICASM0.6018	Chr 1	69681500–69681795	312	103	6.28	11422.81	nucleus	-0.319
SmSAUR14	evm.model.HICASM0.6019	Chr 1	69684559–69684825	267	88	6.27	10090.57	chloroplast	-0.208
SmSAUR15	evm.model.HICASM0.6020	Chr 1	69691882–69692151	270	89	6.83	10163.6	chloroplast	-0.254
SmSAUR16	evm.model.HICASM0.6021	Chr 1	69694065–69694331	267	88	6.27	10105.52	mitochondrion	-0.294
SmSAUR17	evm.model.HICASM0.6022	Chr 1	69700340–69700609	270	89	6.27	10072.49	mitochondrion	-0.181
SmSAUR18	evm.model.HICASM0.6024	Chr 1	69763631–69763957	384	127	8.98	14712.01	chloroplast	-0.247
SmSAUR19	evm.model.HICASM0.6025	Chr 1	69765812–69766063	252	83	5.52	9583.92	chloroplast	-0.257
SmSAUR20	evm.model.HICASM0.6026	Chr 1	69766989–69767258	270	89	6.4	10156.59	chloroplast	-0.112
SmSAUR21	evm.model.HICASM0.6027	Chr 1	69768323–69768589	267	88	5.87	10114.55	mitochondrion	-0.208
SmSAUR22	evm.model.HICASM0.6032	Chr 1	69902535–69902801	267	88	6.82	10050.54	mitochondrion	-0.183
SmSAUR23	evm.model.HICASM0.6034	Chr 1	69928469–69928735	267	88	6.83	10046.5	mitochondrion	-0.198
SmSAUR24	evm.model.HICASM0.6035	Chr 1	69931760–69932029	270	89	6.83	10163.6	chloroplast	-0.254
SmSAUR25	evm.model.HICASM0.6037	Chr 1	69976232–69976546	315	104	7.82	11924.82	chloroplast	-0.347
SmSAUR26	evm.model.HICASM0.6039	Chr 1	70017208–70017606	399	132	9.19	14917.19	chloroplast	-0.177

Chr, chromesome; CDS, coding sequence; bp, base pair; aa, amino acids; pI, isoelectric point; Mw, molecular weight; Da, Dalton.

Gene name	Gene ID	Chromosome	Locus	CDS Length (bp)	Number of aa	Theoretical pI	Mw (Da)	Subcellular localization	Gravy
SmSAUR27	evm.model.HICASM1.5009	Chr 2	63596400–63596828	429	142	10.06	16227.84	mitochondrion	-0.334
SmSAUR28	evm.model.HICASM1.5015	Chr 2	63732051–63732368	318	105	6.9	12058.92	chloroplast	-0.39
SmSAUR29	evm.model.HICASM1.5505	Chr 2	68955041–68955370	330	109	8.45	12995.85	nucleus	-0.601
SmSAUR30	evm.model.HICASM2.1351	Chr 3	23042824–23043052	405	134	9.66	14678.84	chloroplast	-0.294
SmSAUR31	evm.model.HICASM3.97	Chr 4	868604–869098	495	164	10.89	19024.16	nucleus	-0.5
SmSAUR32	evm.model.HICASM3.2820	Chr 4	35597525–35598022	498	165	9.65	18438.09	mitochondrion	-0.398
SmSAUR33	evm.model.HICASM3.2935	Chr 4	37051300–37051656	357	118	5.3	13210.05	nucleus	-0.206
SmSAUR34	evm.model.HICASM3.2939	Chr 4	37090531–37090996	498	165	5.5	18520.99	nucleus	-0.492
SmSAUR35	evm.model.HICASM3.4371	Chr 4	52055715–52056212	498	165	9.3	18433.28	nucleus	-0.099
SmSAUR36	evm.model.HICASM3.4460	Chr 4	52984356–52984656	366	121	9.84	14240.51	mitochondrion	-0.611
SmSAUR37	evm.model.HICASM3.4501	Chr 4	53346802–53347116	315	104	9.64	12002.68	chloroplast	-0.495
SmSAUR38	evm.model.HICASM3.4569	Chr 4	53835866–53836330	465	154	11.07	17607.71	chloroplast	-0.401
SmSAUR39	evm.model.HICASM3.4793	Chr 4	55416083–55416505	423	140	8.74	15644.22	mitochondrion	-0.04
SmSAUR40	evm.model.HICASM3.4794	Chr 4	55418215–55418637	423	140	7.69	15702.95	nucleus	-0.336
SmSAUR41	evm.model.HICASM4.1150	Chr 5	11494668–11495033	366	121	6.83	13768.96	chloroplast	-0.16
SmSAUR42	evm.model.HICASM4.1195	Chr 5	12088748–12089086	339	112	9.07	12823.73	chloroplast	-0.338
SmSAUR43	evm.model.HICASM5.267	Chr 6	2265510–2265944	435	144	8.98	16339.96	nucleus	-0.439
SmSAUR44	evm.model.HICASM5.3617	Chr 6	45409751–45410071	321	106	8.63	12456.22	nucleus	-0.681
SmSAUR45	evm.model.HICASM5.3618	Chr 6	45421236–45421402	243	80	9.34	9135.69	nucleus	-0.586
SmSAUR46	evm.model.HICASM6.2154	Chr 7	20792434–20792823	390	129	6.81	14850.74	nucleus	-0.597
SmSAUR47	evm.model.HICASM7.265	Chr 8	3589444–3589803	360	119	6.29	13511.53	chloroplast	-0.407
SmSAUR48	evm.model.HICASM7.695	Chr 8	7220590–7220940	351	116	6.82	12780.83	nucleus	-0.078
SmSAUR49	evm.model.HICASM7.1146	Chr 8	11859967–11860281	315	104	8.51	11889.73	nucleus	-0.307
SmSAUR50	evm.model.HICASM7.1799	Chr 8	18500227–18500472	246	81	9.06	9473.02	nucleus	-0.347
SmSAUR51	evm.model.HICASM7.3159	Chr 8	32614058–32614429	372	123	9.17	14287.05	chloroplast	-0.088
SmSAUR52	evm.model.HICASM7.3188	Chr 8	32937744–32938100	357	118	7.02	13610.51	nucleus	-0.612
SmSAUR53	evm.model.HICASM7.3191	Chr 8	32957898–32958266	369	122	5.3	13604	nucleus	0.234

Chr, chromesome; CDS, coding sequence; bp, base pair; aa, amino acids; pI, isoelectric point; Mw, molecular weight; Da, Dalton.

Gene name	Gene ID	Chromosome	Locus	CDS Length (bp)	Number of aa	Theoretical pI	Mw (Da)	Subcellular localization	Gravy
SmSAUR54	evm.model.HICASM7.3595	Chr 8	38143478–38143852	375	124	8.26	13579.82	extracellular space	-0.007
SmSAUR55	evm.model.HICASM7.4013	Chr 8	44415884–44416047	393	130	9.02	14332.61	nucleus	-0.218

Chr, chromesome; CDS, coding sequence; bp, base pair; aa, amino acids; pI, isoelectric point; Mw, molecular weight; Da, Dalton.

Localization of *SmSAURs* on the chromosomes was mapped in order to further understand the characteristics of these *SmSAURs*. The positions of *SmSAUR* genes were visualized using TBtools software (Fig. 1). The majority of members (26 *SmSAURs*) were located on chromosome 1, whereas chromosome 3 and chromosome 7 had only one member. The remaining members were arranged according to the distribution of *SmSAUR* genes on the chromosomes: chromosome 2 (3 *SmSAURs*), chromosome 4 (9 *SmSAURs*), chromosome 5 (2 *SmSAURs*), chromosome 6 (2 *SmSAURs*), chromosome 8 (9 *SmSAURs*). In addition, most *SmSAURs* were located in tandem clusters on chromosomes. The largest *SmSAUR* cluster was located on chromosome 1 and contains 19 tandem members, known as SmSAUR8-26. Two *SmSAUR* genes clusters were located on chromosome 4 and have two members (*SmSAUR33* and *SmSAUR34*, *SmSAUR39* and *SmSAUR40*) respectively. The *SmSAUR* gene cluster was composed of two genes on chromosome 1 (*SmSAUR4* and *SmSAUR5*), chromosome 2(*SmSAUR4* and *SmSAUR5*), chromosome 6 (*SmSAUR44* and *SmSAUR45*) and chromosome 8 (*SmSAU52* and *SmSAUR53*).

Phylogenetic, protein motif and conserved domain analysis of SmSAURs

To investigate the evolutionary relationships among the 55 SmSAURs, a phylogenetic tree was constructed based on the multiple alignment of the auxin-inducible domains of *S. miltiorrhiza*, *A. thaliana*, and *O. sativa*, using the neighbor-joining (NJ) method. The 55 SmSAUR proteins were divided into five groups (group Ⅰ-Ⅴ), which contained 39, 7, 4, 2, and 3 proteins, respectively. Majority of the SmSAUR proteins and their homologs in *A. thaliana* were assigned to the same groups, indicating a close evolutionary relationship between SmSAUR and AtSAUR proteins (Fig. 2).

To study the phylogenetic classification and structural diversity of putative SmSAUR proteins, a phylogenetic tree based on the amino acid sequences of SmSAUR proteins was constructed using the NJ method (Fig. 3a). In addition, the motifs in SmSAURs were analyzed using the MEME website. In total, 10 conserved motifs were identified and predicted among the 55 SmSAUR proteins, named Motif 1–10. The consensus sequences and E-value of all sequences were displayed in Table S3. Almost all SmSAUR proteins contained conserved Motif 1, Motif 2, and Motif 3. These three motifs represented the auxin-inducible domain and may play an essential role in the auxin signaling pathway. In addition, Motif 4 and Motif 6 usually appeared at the N-terminal, while Motif 3 and Motif 7 appeared at the C-terminal (Fig. 3b). The results indicated that the SmSAUR family domains were highly conserved in evolution, and closely related members of the phylogenetic tree contained the same motifs. Subsequently, the conserved domains of 55 SmSAUR proteins were analyzed. All SmSAUR proteins have a typical auxin-inducible or auxin-inducible superfamily domain (Fig. 3c). Auxin-inducible proteins and auxin-inducible superfamily proteins share a common ancestor in evolution, indicating that they belong to the same family. This confirms that these SmSAUR proteins are part of the same family.

Analysis related cis-acting elements and gene structure of the SmSAURs

In order to intuitively understand the characteristics of *SmSAUR* genes, the phylogenetic tree of SmSAUR proteins were constructed (Fig. 4a). To understand the potential functions of the *SmSAUR* genes in response to various reactions, we selected 2 kilobase promoter regions from the transcription start sites for *cis*-acting elements analysis (Fig. 4b). The *cis*-acting elements can be categorized into three primary categories: phytohormone response, abiotic and biological stress, as well as plant growth and development. In this study, many *cis*-acting elements related to phytohormone response were identified. A total of 39 auxin response elements, 57 MeJA response elements, 75 ABA response elements, 49 GA response elements and 31 SA response elements were identified in 55 *SmSAURs*. With the exception of *SmSAUR25* and *SmSAUR46*, all promoters included phytohormone response elements. In particular, the promoter sequences of *SmSAUR10* and *SmSAUR40* contained 3–4 auxin response elements, suggesting that these two genes played important roles in the response to auxin in *S. miltiorrhiza*. In addition, 6 *cis*-acting elements related to abiotic and biological stress, as well as 3 *cis*-acting elements related to plant growth and development, were also identified. With the exception of SmSAUR25 and SmSAUR46, all promoters included phytohormone response elements. It was estimated that 33 *SmSAURs* were involved in plant growth and development. In conclusion, *SmSAUR* genes are likely to participate in various hormonal regulations, stress responses, as well as plant growth and development.

By analyzing the exon/intron structure of *SmSAUR* genes, we found that all *SmSAUR* genes had complete open reading frame (ORF). Among them, 9 *SmSAURs* (*SmSAUR13*, *SmSAUR18*, *SmSAUR30*, *SmSAUR55*, *SmSAUR4*, *SmSAUR34*, *SmSAUR2*, *SmSAUR45*, and *SmSAUR36*) contained one intron, while the remaining genes comprised a single exon without any introns (Fig. 4c). These results were consistent with the typical characteristics of the *SAUR* gene family.

Synteny analysis of SAURs

In order to comprehend the underlying genetic mechanisms in evolution, an analysis of gene duplication events was performed on the *SmSAUR* gene family in *S. miltiorrhiza*. Five tandem duplication events revealed the clustering of 15 *SmSAUR* genes: *SmSAUR4/34*, *SmSAUR5/33*, *SmSAUR6/32*, *SmSAUR9/25/49*, *SmSAUR31/38* and *SmSAUR36/47/48/52* (Fig. 5a). In addition to tandem duplication events, we identified 11 pairs of segmental duplication events using BLASTP and MCScanX methods. These findings indicated that gene duplication likely played a significant role in the generation of

most *SmSAUR* genes, with tandem duplication events serving as the primary driving force for gene evolution. To gain a deeper understanding of the phylogenetic mechanisms among *SmSAUR* genes, two comparative syntenic maps were created for *S. miltiorrhiza*, associating it with two representative species: dicotyledonous (*A. thaliana*) and monocotyledonous (*O. sativa*) plants. (Fig. 5b). The results showed that there were 40 homologous gene pairs between *S. miltiorrhiza* and *A. thaliana*, which were distributed on all chromosomes except chromosome 3. There were 12 homologous gene pairs between *S. miltiorrhiza* and *O. sativa*, distributed on chromosomes 1, 4, 5, and 6. More gene duplication events revealed the high homology between *S. miltiorrhiza* and *A. thaliana*.

Expression profiles of SmSAUR genes in different organs of S. miltiorrhiza

To assess the tissue-specific expression patterns of *S. miltiorrhiza SAUR* genes, we analyzed the transcriptome data from root, stem, leaf, and flower. After removing low-quality reads and adapters, the sequencing of root, stem, leaf, and flower samples produced 48.03 million, 47.29 million, 49.84 million, and 44.03 million clean reads, respectively (Table S5). To verify the reliability and validity of the experiment, principal component analysis (PCA) was performed. The results of the PCA indicated significant separation among the various treatment groups (Fig. S1a). To ensure comparability of gene expression estimates across different experiments, we employed the most widely used gene expression normalization method. This method calculates the transcripts per kilobase per million mapped reads (TPM) value for each gene, taking into account the effects of sequencing depth and gene length on read counts, thereby normalizing the expression levels of all genes. The analysis results of gene expression levels displayed that the $\log_{10}^{(TPM+1)}$ values of all annotated genes were distributed between − 1.50 and 3.50 in root, stem, flower and leaf sample group, and most genes were closely clustered between 0.50 and 1.50 (Fig. S1b). A Venn diagram was generated based on the comparative results of all annotated genes in root, stem, leaf, and flower. Venn diagram displayed the 18,039 overlapped expressed genes between root and leaf group, 18,765 overlapped expressed genes in root group and stem group, 18,136 overlapped genes in root group and flower group, 18,854 overlapped genes in leaf group and stem group, 18,400 overlapped genes in leaf group and flower group, 18,890 overlapped genes in flower group and stem group, and 17,174 overlapped expressed genes in root, stem, leaf, and flower groups (Fig. S1c).

The transcripts of 1 *SmSAUR* gene (*SmSAUR35*) were not detected in any of these 12 samples, indicating that *SmSAUR35* was either pseudogene or had special expression pattern that was not examined in our libraries. 54 *SmSAUR* genes were expressed in all 12 samples tested (FPKM > 0), and 35 genes showed constitutive expression (FPKM > 2 in all samples). The expression profiles of *SmSAURs* indicated that *SmSAUR13*, *SmSAUR31* and *SmSAUR46* were highly expressed in all organs selected in this study, suggesting that these 3 genes were key functional genes (Fig. 6a). Analysis of expression profiles revealed that 29 *SmSAURs* exhibited the highest expression in flowers, while 5 members, namely *SmSAUR26*, *SmSAUR31*, *SmSAUR32*, *SmSAUR36*, and *SmSAUR43*, exhibited the highest expression levels in roots. *SmSAURs* with a close evolutionary relationship had similar expression characteristics. For example, *SmSAUR15*, *SmSAUR17*, *SmSAUR10*, *SmSAUR23*, *SmSAUR24*, *SmSAUR16*, *SmSAUR21*, *SmSAUR10*, and *SmSAUR18* all had the lowest expression levels in the roots and the highest expression levels in the flowers. The expression levels of *SmSAUR33*, *SmSAUR41*, *SmSAUR42*, *SmSAUR43*, and *SmSAUR54*, which were closely related to evolution, were the lowest in the leaves. Additionally, primer details were provided in Table S4, and qRT-PCR was conducted to validate the expression levels of selected genes, with results consistent with the transcriptome sequencing data (Fig. 6b-i). The expression levels of *SmSAURs* in the four organs were notably different, indicating that they may have multiple functions during the growth and development of *S. miltiorrhiza*.

Exogenous IAA promoted the growth and root development in S. miltiorrhiza in hydroponic culture

To elucidate the relationship between *SmSAUR* genes and IAA, seedlings of this herb were treated with 0.10 μmol·L^{-1} IAA, and the phenotypic indexes of the IAA-treated and control groups were determined. The results indicated that IAA positively regulated the growth and root development in *S. miltiorrhiza* (Fig. 7b). The IAA treatment group exhibited increased counts of primary lateral roots, secondary lateral roots, diameter of primary lateral roots, root biomass, and fresh weight of the above-ground portion. However, there was no significant ($P < 0.05$) difference in plant height and leaf number between the IAA-treated and control groups (Fig. 7b-i). Specifically, the number of primary lateral roots, number of secondary lateral roots, diameter of primary lateral roots, root biomass, and fresh weight of the above-ground portion were 1.52-fold, 2.42-fold, 1.33-fold, 1.55-fold and 1.28-fold of that in the control group, respectively.

Screening SmSAUR genes involved in root development of salvia miltiorrhiza was based on Pearson correlation coefficient

In order to identify auxin regulated *SmSAURs* that may be involved in root development, root samples of the IAA-treated and control groups were analyzed by RNA-seq based on the experimental results of IAA promoting root development of *S. miltiorrhiza*. As the results shown in Table S6, there were 49.33 million raw reads and 48.84 million clean reads in the control group, and 49.78 million raw reads and 49.28 million clean reads in the IAA group. In addition, as shown in the Venn diagram, there is 19,723 overlapped expressed genes between the two groups (Fig. 7a). The expression distribution of genes based on TPM values, the statistical results of gene expression distribution showed that the $\log_{10}^{(TPM+1)}$ values of most annotated genes were closely clustered between 0.50 and 2.00 in both the IAA-treated and control groups (Fig. 7b). $|\log_2^{(\text{Fold change})}| \geq 1$ and $P < 0.05$ were used as the default thresholds to screen the differentially expressed genes (DEGs) in the IAA group, there were 1933 differential statistics in the IAA-treated and control groups, including 994 upregulated genes and 939 downregulated genes (Fig. 7c, Table S7). All the DEGs were approximately symmetrical in the Volcano plot and the hierarchical clustering were presented in a heatmap according to the markedly different values of $-\log_{10}^{(P\text{ adjusted})}$ and $\log_2^{(\text{Fold Chang})}$ (Fig. 7d).

All *SmSAUR* genes in the transcriptome data were screened, and the gene expression levels were visualized using a heatmap generated by TBtools software according to the $\log_2^{(TPM+1)}$ values. The analysis results showed that there were 27 up-regulated *SmSAUR* genes in the IAA group, among which the expression levels of *SmSAUR9* and *SmSAUR18* increased most significantly. In addition, 20 down-regulated *SmSAURs* were screened in the IAA group

and the most prominent ones were *SmSAUR6*, *SmSAUR30*, *SmSAUR33*, *SmSAUR40*, and *SmSAUR55*. But the expression levels of *SmSAUR22*, *SmSAUR14*, *SmSAUR19*, *SmSAUR50*, *SmSAUR1*, *SmSAUR2*, *SmSAUR45*, and *SmSAUR47* was no significant change, indicating that they were not regulated by IAA (Fig. 8a). Besides, the expression of some of the aforementioned genes were also determined by qRT-PCR using the primers listed in Table S4, the results were consistent with the transcriptome sequencing data (Fig. 8b).

To further clarify the role of *SmSAUR* genes in root development of *S. miltiorrhiza*, Pearson correlation coefficient analysis was used according to transcriptome-based data. As shown in Fig. 9 and Table S8, the fresh weight of root was positively correlated with the expression level of *SmSAUR38* ($P < 0.05$) and showed an extremely negative correlation with *SmSAUR28* ($P < 0.01$). There was no significant correlation between the primary lateral root number and the expression of the *SmSAUR* genes. The secondary lateral root number showed an extremely positive correlation with *SmSAUR18* ($P < 0.01$) and a negative correlation with *SmSAUR4* ($P < 0.05$). The diameter of the primary lateral root showed a positive association with *SmSAUR4* ($P < 0.05$). The last one, root length was extremely positively correlated with *SmSAUR28* ($P < 0.01$) and positively correlated with *SmSAUR37* ($P < 0.05$), while it was negatively correlated with *SmSAUR38* ($P < 0.05$). According to these results, it is speculated that several *SmSAUR* members may play distinct roles in regulating auxin-mediated root development in *S. miltiorrhiza*.

Disscussion

The genome-wide characterization and bioinformatic analysis of *SmSAURs* can enhance our understanding of their regulatory roles in the growth and development of *S. miltiorrhiza*. Previous studies have indicated that most plant genomes typically contain 50 to 140 members of the *SAUR* gene family, and it is generally observed that *SAUR* genes lack introns (Zhang, et al. 2021). In this study, a total of 55 *SmSAUR* members were identified. Most of these members was not contained introns and were unevenly distributed on 8 chromosomes. The theoretical pI values of *SmSAURs* ranged from 4.99 to 11.07. This result was similar to the previous studies. In *Pyrus bretschneideri*, *Benincasa hispida*, and *Setaria italica*, theoretical pI values range from 5.10 to 10.28, from 4.60 to 10.67, and from 4.90 to 11.61, respectively (Luo, et al. 2022; Ma, et al. 2023; Wang, et al. 2022). Nearly all SmSAUR proteins exhibited hydrophilic properties. This finding was consistent with previous findings, Wang, et, al. (2022) reveal that all the PbrSAUR proteins are hydrophilic (Wang, et al. 2022). Replication gene pairs had the potential to facilitate the expansion of the *SAUR* gene family and enhanced their functional diversity. This study revealed the occurrence of 5 tandem duplication events and 11 pairs of segmental duplication events among *SmSAURs*. Additionally, synteny analysis demonstrate the presence of a significant number of *SAUR* homologous gene pairs in *S. miltiorrhiza*, *A. thaliana*, and *O. sativa*. Likewise, *SAURs* undergo gene expansion events, resulting in the presence of 113, 21, and 28 gene pairs in *Arachis hypogaea*, *P. bretschneideri*, and *Arachis duranensis*, respectively (Liu, et al. 2022; Wang, et al. 2022; Zhuang, et al. 2019). A total of 33 tandem duplication events and 9 segment duplication pairs were identified in *SiSAURs* from *S. italica*, which exhibit collinearity with 4 *A. thaliana* genes and 18 *O. sativa* genes (Ma, et al. 2023).

As a class of genes that rapidly and violently respond to auxin, *SAURs* usually contain a variety of auxin response elements in their promoter sequences. The promoters of *AcoSAURs* from *Ananas comosus* exhibit the presence of five key auxin-responsive elements: Dof protein binding element, AuxRE element, ARF binding element, NDE element, and ASF-1 binding element. Among these elements, *AcoSAUR9* has 10 auxin response elements (Zhang, et al. 2023). The promoters of 18 *SiSAURs* from *S. italica* were found to contain the AuxRR-core element, while the promoters of 31 *SiSAURs* were found to contain the TGA-box element (Ma, et al. 2023). Luan et al (2023) found that *CsSAURs* contain multiple auxin response elements, including 12 TGA-elements, 6 AuxRE elements, and 2 AuxRR-core elements in *Cucumis sativus*. This study also arrived at a similar conclusion. The promoter region of *ZmSAUR8* in *Zea mays* was found to harbor 4 ASF-1 binding elements and 1 AuxRE element, and subsequent IAA treatment resulted in a significant upregulation of *ZmSAUR8* expression (Chen, et al. 2014). In *Citrullus lanatus*, *ClaSAUR44* contains 4 AuxRE elements and 2 NDE elements. After application of IAA treatment, the expression of *ClaSAUR44* is slightly down-regulated (Zhang, et al. 2017). Consistent with previous report, analysis of *cis*-acting elements revealed the presence of auxin response elements, such as TGA-elements, AuxRE, and AuxRR-core, in a total of 29 *SmSAURs*. Subsequent analysis revealed significant regulation of *SmSAURs* (*SmSAUR10*, *SmSAUR11*, *SmSAUR23*, *SmSAUR32*, *SmSAUR40*, *SmSAUR48*, and *SmSAUR49*), which exhibited a high abundance of auxin response elements, following IAA treatment. These results indicated that *SmSAURs* were highly likely to possess momentous roles in modulating the IAA response in *S. miltiorrhiza*.

SAURs exhibit a high degree of functional diversity in regulating plant growth and development, with their gene expression patterns closely associated with their respective functions. For instance, *AtSAUR53* is expressed in the cotyledon and upper hypocotyl of *A. thaliana* seedlings, and its overexpression leads to seedlings with enlarged cotyledons and elongated hypocotyls (Kathare, et al. 2018). In *O. sativa*, the expression of *OsSAUR56* is higher in inflorescence, and knock-out of *OsSAUR56* promotes flowering (Zhao, et al. 2023). *CsSAUR31* has a high expression level in the root, and overexpression of *CsSAUR31* increases the root length of *Cucumis sativus* (Luan, et al. 2023). In this study, the expression analysis revealed that *SmSAUR31, SmSAUR26, SmSAUR32, SmSAUR41*, and *SmSAUR43* all had the highest expression in the roots. Among them, the expression of *SmSAUR26* and *SmSAUR32* in the root is much higher than that in other organs. These results indicate that these *SmSAUR* genes may be involved in the physiological process of root development in *S. miltiorrhiza*.

As the early auxin-response genes, *SAURs* play a crucial role in auxin signal transduction. Numerous studies have demonstrated that the expression of *SAURs* is induced by exogenous auxin. Liu et al. (2022) report that *AhSAURs* from different subfamilies exhibit distinct expression characteristics in response to IAA. Notably, the expression levels of most members in subfamily II and subfamily III are up-regulated and peak after 30 minutes of IAA treatment in *A. hypogaea*. In *Medicago truncatula*, *MtSAUR* genes containing more than two AuxRE elements display rapid responsiveness to exogenous IAA within 5 minutes (Zhang, et al. 2021). In *Malus domestica*, the expressions of 42 *MdSAURs* is down-regulated, while 16 genes are up-regulated after the application of 10 $mmol \cdot L^{-1}$ IAA (Wang, et al. 2020). Similarly, in this study, the expression levels of most *SmSAURs* were regulated after being treated with exogenous IAA. These results implied that these *SmSAUR* members may play specific roles in the IAA signaling transduction pathway. In addition, previous investigation suggests that *SAURs* participate in auxin-regulated plant root development. Overexpression of *AtSAUR53* in *A. thaliana* leads to

elongated and curly primary roots, potentially interfering with auxin transport (Kathare, et al. 2018). The PagWOX11/12a-PagSAUR36 module positively regulates the number and length of adventitious roots through the IAA signaling pathway in *Populus* (Liu, et al. 2022). The expression level of *CbSAUR41* is up-regulated and positively correlated with the formation of lateral root initiation sites and the elongation of root cells under indole-3-butyric acid (IBA) treatment in *Cinnamomum bodinieri* (Xiao, et al. 2020). Consistent with these findings, our study demonstrated that *S. miltiorrhiza* seedlings exhibited an increasing in root biomass, more lateral roots, and thicker root diameter following IAA treatment. Correlation analysis between genes expressions and root morphological indexes revealed that the *SmSAURs* were closely associated with root development of *S. miltiorrhiza*, and several members of *SmSAURs* were found to be significantly correlated with two or more root morphological indexes simultaneously. There was a positive correlation between the fresh weight of the root and the expression level of *SmSAUR38*, while exhibited an extremely negative correlation with *SmSAUR28*. The number of secondary lateral roots exhibited an extremely positive correlation with *SmSAUR18* and a negative correlation with *SmSAUR4*. The diameter of the primary lateral root exhibited a positive association with *SmSAUR4*. Lastly, the root length exhibited an extremely positive correlation with *SmSAUR28* and a positive correlation with *SmSAUR37*, but it showed a negative correlation with *SmSAUR38*. These highly correlated *SmSAUR* genes can be considered as primary candidate genes regulating root development in *S. miltiorrhiza*.

Conclusions

The *SAUR* gene family plays an indispensable role in regulating diverse biological processes in plants. In this study, we identified and analyzed 55 *SmSAURs*. Chromosomal mapping showed that 55 *SmSAUR* genes were distributed on all 8 chromosomes of *S. miltiorrhiza*, and gene clusters were present. Phylogenetic analysis demonstrated the clustering of *SmSAURs* into 5 distinct groups. Gene structure and motif analyses revealed that the majority of *SmSAURs* exhibited a conventional distribution of exons and introns, along with consistent motif compositions. Synteny analysis results demonstrated that *SmSAURs* and *AtSAURs* experienced multiple gene duplication events. Diverse *cis*-acting elements were identified in the promoter of *SmSAUR* genes, with hormone-responsive elements accounting for a high proportion. Tissue-specific analysis revealed alterations in the expression levels of 55 members of *SmSAUR* gene family across four distinct organs. Based on the RNA-seq data from *S. miltiorrhiza* seedlings treated with IAA, combined with Pearson correlation coefficient analysis, we found that several root morphological indexes were correlated with the expression of *SmSAURs*. Namely, the diameter of primary lateral root was positively correlated with *SmSAUR4*. The secondary later root number was positively correlated with *SmSAUR18* and negatively correlated with *SmSAUR4*. The root length showed a positive correlation with *SmSAUR28* and *SmSAUR37* and a negative correlation with *SmSAUR38*. The root fresh biomass exhibited a positive correlation with *SmSAUR38* and a negative correlation with *SmSAUR28*. *SmSAUR4*, *SmSAUR18*, *SmSAUR28*, *SmSAUR37*, and *SmSAUR38* could be used as the potential candidates in the future study to uncover the molecular mechanism underlying the auxin-mediated root development in *S. miltiorrhiza*.

Declarations

Funding

This work was financially supported by the National Natural Science Foundation of China (31700257), Key project at central government level: The ability establishment of sustainable use for valuable Chinese medicine resources (2060302), Independent Innovation Fund Project of Agricultural Science and Technology in Jiangsu Province (CX(23)3113), Science and Technology Development Project of Traditional Chinese Medicine in Jiangsu Province (MS2022154), Zhejiang Provincial Natural Science Foundation of China (LR21H280002), the Major Science and Technology Projects of Breeding New Varieties of Agriculture in Zhejiang Province (2021C02074), and Postgraduate Research & Practice Innovation Program of Jiangsu Province (KYCX22_3473).

Competing Interests

The authors have no relevant financial or non-financial interests to disclose.

Author contributions

SCZ and DFY conceptualized and designed the work. WW, YWZ, and ZYZ conducted the experiments. WW, LQ, and YYG contributed to data analysis. WW and SCZ drafted the manuscript. RM and HGZ provided critical comments to the manuscript. All authors have read and approved the final manuscript.

Data availability

The datasets generated during the study are accessible in the Sequence Read Archive (SRA) database of the National Center for Biotechnology Information (NCBI) under the accession PRJNA1069646 and accession PRJNA1069996.

Ethical approval

This article does not contain any studies with human participants or animals performed by any of the authors.

References

1. Altschul SF, Madden TL, Schaeffer AA, Zhang JH, Zhang Z, Miller W, Lipman DJ (1997) Gapped BLAST and PSI-BLAST: A new generation of protein database search programs. Nucleic Acids Res 25:3389–3402. https://doi.org/10.1093/nar/25.17.3389

2. Anai T, Kono N, Kosemura S, Yamamura S, Hasegawa K (1998) Isolation and characterization of an auxin-inducible *SAUR* gene from radish seedlings. DNA Seq 9:329–333. https://doi.org/https://doi.org/10.3109/10425179809008472
3. Bailey TL, Boden M, Buske FA, Frith M, Grant CE, Clementi L, Ren J, Li WW, Noble WS (2009) MEME SUITE: tools for motif discovery and searching. Nucleic Acids Res 37:W202–W208. https://doi.org/10.1093/nar/gkp335
4. Bennett J, Hondred D, Register JC (2015) Keeping qRT-PCR rigorous and biologically relevant. Plant Cell Rep 34:1–3. https://doi.org/10.1007/s00299-014-1692-6
5. Cao Y, Chen R, Wang WT, Wang DH, Cao XY (2021) SmSPL6 induces phenolic acid biosynthesis and affects root development in *Salvia miltiorrhiza*. Int J Mol Sci 22:7895. https://doi.org/10.3390/ijms22157895
6. Chen CJ, Wu Y, Li JW, Wang X, Zeng ZH, Xu J, Liu YL, Feng JT, Chen H, He YH, Xia R (2023) TBtools-II: A one for all, all for one bioinformatics platform for biological big-data mining. Mol Plant 16:1733–1742. https://doi.org/10.1016/j.molp.2023.09.010
7. Chen YZ, Hao X, Cao J (2014) *Small auxin up-regulated RNA* (*SAUR*) gene family in maize: Identification, evolution, and its phylogenetic comparison with *Arabidopsis*, rice, and sorghum. J Integr Plant Biol 56:133–150. https://doi.org/10.1111/jipb.12127
8. Gasteiger E, Hoogland C, Gattiker A, Duvaud Se, Wilkins MR, Appel RD, Bairoch A (2005) Protein identification and analysis tools on the ExPASy server. In: Walker JM (ed) The Proteomics Protocols Handbook. Humana, Totowa, NJ, pp 571–607
9. Guo Y, Jiang QY, Hu Z, Sun XJ, Fan SJ, Zhang H (2018) Function of the auxin-responsive gene *TaSAUR75* under salt and drought stress. Crop J 6:181–190. https://doi.org/10.1016/j.cj.2017.08.005
10. Hu B, Jin JP, Guo AY, Zhang H, Luo JC, Gao G (2014) GSDS 2.0: an upgraded gene feature visualization server. Bioinformatics 31:1296–1297. https://doi.org/10.1093/bioinformatics/btu817
11. Hu WF, Yan HW, Luo SS, Pan F, Wang Y, Xiang Y (2018) Genome-wide analysis of poplar *SAUR* gene family and expression profiles under cold, polyethylene glycol and indole-3-acetic acid treatments. Plant Physiol Biochem 128:50–65. https://doi.org/10.1016/j.plaphy.2018.04.021
12. Jain M, Tyagi AK, Khurana JP (2006) Genome-wide analysis, evolutionary expansion, and expression of early auxin-responsive *SAUR* gene family in rice (*Oryza sativa*). Genomics 88:360–371. https://doi.org/10.1016/j.ygeno.2006.04.008
13. Kathare PK, Dharmasiri S, Dharmasiri N (2018) *SAUR53* regulates organ elongation and apical hook development in *Arabidopsis*. Plant Signal Behav 13:e1514896. https://doi.org/10.1080/15592324.2018.1514896
14. Kong YY, Zhu YB, Gao C, She WJ, Lin WQ, Chen Y, Han N, Bian HW, Zhu MY, Wang JH (2013) Tissue-specific expression of *SMALL AUXIN-UP RNA41* differentially regulates cell expansion and root meristem patterning in *Arabidopsis*. Plant Cell Physiol 54:609–621. https://doi.org/10.1093/pcp/pct028
15. Lee SR, Jeon H, Kwon JE, Suh H, Kim BH, Yun MK, Lim YJ, Kang SC (2020) Anti-osteoporotic effects of *Salvia miltiorrhiza* Bunge EtOH extract both in ovariectomized and naturally menopausal mouse models. J Ethnopharmacol 258:112874. https://doi.org/10.1016/j.jep.2020.112874
16. Li HY, Liu TR, Wang B, Li HB (2022) Genome-wide characterization and expression analysis of *GATA* transcription factors in response to methyl jasmonate in *Salvia miltiorrhiza*. Genes 13:822. https://doi.org/10.3390/genes13050822
17. Lin YL, Wu CH, Luo MH, Huang YJ, Wang CN, Shiao MS, Huang YT (2006) In vitro protective effects of salvianolic acid B on primary hepatocytes and hepatic stellate cells. J Ethnopharmacol 105:215–222. https://doi.org/10.1016/j.jep.2005.10.021
18. Liu R, Wen SS, Sun TT, Wang R, Zuo WT, Yang T, Wang C, Hu JJ, Lu MZ, Wang LQ (2022) PagWOX11/12a positively regulates the *PagSAUR36* gene that enhances adventitious root development in poplar. J Exp Bot 73:7298–7311. https://doi.org/10.1093/jxb/erac345
19. Liu YY, Xiao LN, Chi JX, Li RC, Han Y, Cui F, Peng ZY, Wan SB, Li GW (2022) Genome-wide identification and expression of *SAUR* gene family in peanut (*Arachis hypogaea* L.) and functional identification of *AhSAUR3* in drought tolerance. BMC Plant Biol 22:178. https://doi.org/10.1186/s12870-022-03564-2
20. Livak KJ, Schmittgen TD (2001) Analysis of relative gene expression data using Real-Time quantitative PCR and the $2^{-\Delta\Delta CT}$ method. Methods 25:402–408. https://doi.org/10.1006/meth.2001.1262
21. Lu XY, Liang XY, Li X, Shen PX, Cao XY, Chen C, Song SH, Wang DH, Wang ZZ, Zhang Y (2020) Genome-wide characterisation and expression profiling of the *LBD* family in *Salvia miltiorrhiza* reveals the function of *LBD50* in jasmonate signaling and phenolic biosynthesis. Ind Crops Prod 144:112006. https://doi.org/10.1016/j.indcrop.2019.112006
22. Luan J, Xin M, Qin ZW (2023) Genome-wide identification and functional analysis of the roles of *SAUR* gene family members in the promotion of cucumber root expansion. Int J Mol Sci 24:5940. https://doi.org/10.3390/ijms24065940
23. Luo C, Yan JQ, He CX, Liu WR, Xie DS, Jiang B (2022) Genome-wide identification of the *SAUR* gene family in wax gourd (*Benincasa hispida*) and functional characterization of *BhSAUR60* during fruit development. Int J Mol Sci 23:14021. https://doi.org/10.3390/ijms232214021
24. Ma XQ, Dai ST, Qin N, Zhu CC, Qin JF, Li JX (2023) Genome-wide identification and expression analysis of the *SAUR* gene family in foxtail millet (*Setaria italica* L). BMC Plant Biol 23:31. https://doi.org/10.1186/s12870-023-04055-8
25. Pan X, Chang YJ, Li C, Qiu XX, Cui XY, Meng FQ, Zhang SX, Li XE, Lu SF (2023) Chromosome-level genome assembly of *Salvia miltiorrhiza* with orange roots uncovers the role of *Sm2OGD3* in catalyzing 15,16-dehydrogenation of tanshinones. Hortic Res 10:uhad069. https://doi.org/10.1093/hr/uhad069
26. Ren H, Gray WM (2015) SAUR proteins as effectors of hormonal and environmental signals in plant growth. Mol Plant 8:1153–1164. https://doi.org/10.1016/j.molp.2015.05.003

27. Ren J, Fu L, Nile SH, Zhang J, Kai GY (2019) *Salvia miltiorrhiza* in treating cardiovascular diseases: A review on its pharmacological and clinical applications. Front Pharmacol 10:753. https://doi.org/10.3389/fphar.2019.00753
28. Savojardo C, Martelli Pier L, Fariselli P, Profiti G, Casadio R (2018) BUSCA: an integrative web server to predict subcellular localization of proteins. Nucleic Acids Res 46:W459–W466. https://doi.org/10.1093/nar/gky320
29. Stortenbeker N, Bemer M (2019) The *SAUR* gene family: the plant's toolbox for adaptation of growth and development. J Exp Bot 70:17–27. https://doi.org/10.1093/jxb/ery332
30. Sun N, Wang J, Gao Z, Dong J, He H, Terzaghi W, Wei N, Deng XW, Chen H (2016) *Arabidopsis SAURs* are critical for differential light regulation of the development of various organs. 113:6071–6076. https://doi.org/doi:10.1073/pnas.1604782113
31. van Mourik H, van Dijk ADJ, Stortenbeker N, Angenent GC, Bemer M (2017) Divergent regulation of *Arabidopsis SAUR* genes: a focus on the *SAUR10*-clade. BMC Plant Biol 17:245. https://doi.org/10.1186/s12870-017-1210-4
32. Wang J, Chitsaz F, Derbyshire MK, Gonzales NR, Gwadz M, Lu S, Marchler GH, Song JS, Thanki N, Yamashita RA, Yang M, Zhang D, Zheng C, Lanczycki CJ, Marchler-Bauer A (2023) The conserved domain database in 2023. Nucleic Acids Res 51:D384–d388. https://doi.org/10.1093/nar/gkac1096
33. Wang K, Cheng YT, Yi L, He HL, Zhan SF, Yang P (2021) Genome-wide identification of the Tubby-Like Protein (TLPs) family in medicinal model plant *Salvia miltiorrhiza*. PeerJ 9:e11403. https://doi.org/10.7717/peerj.11403
34. Wang LL, Ma RF, Liu CY, Liu HX, Zhu RY, Guo SZ, Tang MK, Li Y, Niu JZ, Fu M, Gao SH, Zhang DW (2017) *Salvia miltiorrhiza*: A potential red light to the development of cardiovascular diseases. Curr Pharm Des 23:1077–1097. https://doi.org/10.2174/1381612822666161010105242
35. Wang MN, Manzoor MA, Wang XY, Feng XF, Zhao Y, He JL, Cai YP (2022) Comparative genomic analysis of *SAUR* gene family, cloning and functional characterization of two genes (*PbrSAUR13* and *PbrSAUR52*) in *Pyrus bretschneideri*. Int J Mol Sci 23:7054. https://doi.org/10.3390/ijms23137054
36. Wang P, Lu SX, Xie M, Wu MD, Ding SL, Khaliq A, Ma ZH, Mao J, Chen BH (2020) Identification and expression analysis of the *small auxin-up RNA* (*SAUR*) gene family in apple by inducing of auxin. Gene 750:144725. https://doi.org/10.1016/j.gene.2020.144725
37. Wang ZP, Zhang ZB, Zheng DY, Zhang TT, Li XL, Zhang C, Yu R, Wei JH, Wu ZY (2022) Efficient and genotype independent maize transformation using pollen transfected by DNA-coated magnetic nanoparticles. J Integr Plant Biol 64:1145–1156. https://doi.org/10.1111/jipb.13263
38. Wilkins MR, Gasteiger E, Bairoch A, Sanchez JC, Williams KL, Appel RD, Hochstrasser DF (1999) Protein identification and analysis tools in the ExPASy server. Methods Mol Biol 112:531–552. https://doi.org/10.1385/1-59259-584-7:531
39. Wu YH, Wu YR, Li B, Yan ZY (2020) Cryptotanshinone: A review of its pharmacology activities and molecular mechanisms. Fitoterapia 145:104633. https://doi.org/10.1016/j.fitote.2020.104633
40. Xiao ZF, Jin ZN, Zhang BH, Li F, Yu FX, Zhang HY, Lü XW, Zhang J (2020) Effects of IBA on rooting ability of *Cinnamomum bodinieri* citral type micro-shoots from transcriptomics analysis. Plant Biotechnol Rep 14:467–477. https://doi.org/10.1007/s11816-020-00626-5
41. Xie JM, Chen YR, Cai GJ, Cai RL, Hu Z, Wang H (2023) Tree Visualization By One Table (tvBOT): a web application for visualizing, modifying and annotating phylogenetic trees. Nucleic Acids Res 51:W587–W592. https://doi.org/10.1093/nar/gkad359
42. Xu YX, Xiao MZ, Liu Y, Fu JL, He Y, Jiang DA (2017) The *small auxin-up RNA OsSAUR45* affects auxin synthesis and transport in rice. Plant Mol Biol 94:97–107. https://doi.org/10.1007/s11103-017-0595-7
43. Xu ZC, Ji AJ, Song JY, Chen SL (2016) Genome-wide analysis of auxin response factor gene family members in medicinal model plant *Salvia miltiorrhiza*. Biol Open 5:848–857. https://doi.org/10.1242/bio.017178
44. Yu H, Chen M, Hu Y, Ou S, Yu X, Liang S, Li N, Yang M, Kong X, Sun C, Jia S, Zhang Q, Liu L, Hurst LD, Li R, Wang W, Wang J (2022) Dynamic reprogramming of H3K9me3 at hominoid-specific retrotransposons during human preimplantation development. Cell Stem Cell 29:1031–1050. e1012 https://doi.org/10.1016/j.stem.2022.06.006
45. Zhang H, Yu ZJ, Yao XD, Chen JL, Chen X, Zhou HW, Lou YX, Ming F, Jin Y (2021) Genome-wide identification and characterization of *small auxin-up RNA* (*SAUR*) gene family in plants: evolution and expression profiles during normal growth and stress response. BMC Plant Biol 21:4. https://doi.org/10.1186/s12870-020-02781-x
46. Zhang N, Huang X, Bao YN, Wang B, Zeng HX, Cheng WS, Tang M, Li YH, Ren J, Sun YH (2017) Genome-wide identification of *SAUR* genes in watermelon (*Citrullus lanatus*). Physiol Mol Biol Plants 23:619–628. https://doi.org/10.1007/s12298-017-0442-y
47. Zhang SC, Qiu L, Zheng YW, Wang W, Zhao HG, Yang DF (2023) Comparative transcriptome analysis reveals the regulatory effects of exogenous auxin on lateral root development and tanshinone accumulation in *Salvia miltiorrhiza*. Planta 258:33. https://doi.org/10.1007/s00425-023-04193-1
48. Zhang T, Jiang B, Xie RX, Xu MF, Li HL, Liu KD (2021) Genome-wide identification and analysis of *Medicago truncatula* s*mall auxin upregulated RNA* (*SAUR*) gene family uncover their roles in nodule formation. J Plant Biochem Biotechnol 30:126–137. https://doi.org/10.1007/s13562-020-00576-7
49. Zhang YF, Ye T, She ZY, Huang SP, Wang LL, Aslam M, Qin RJ, Wang XY, Qin Y, Niu XP (2023) *Small Auxin Up RNA* (*SAUR*) gene family identification and functional genes exploration during the floral organ and fruit developmental stages in pineapple (*Ananas comosus* L.) and its response to salinity and drought stresses. Int J Biol Macromol 237:124061. https://doi.org/10.1016/j.ijbiomac.2023.124061
50. Zhao Z, Chen TK, Yue JC, Pu N, Liu JZ, Luo LX, Huang M, Guo T, Xiao WM (2023) *Small Auxin Up RNA 56* (*SAUR56*) regulates heading date in rice. Mol Breed 43:62. https://doi.org/10.1007/s11032-023-01409-w
51. Zhu Z, Yogev U, Keesman KJ, Rachmilevitch S, Gross A (2023) Integrated hydroponics systems with anaerobic supernatant and aquaculture effluent in desert regions: Nutrient recovery and benefit analysis. Sci Total Environ 904:166867. https://doi.org/10.1016/j.scitotenv.2023.166867
52. Zhuang WJ, Chen H, Yang M, Wang JP, Pandey MK, Zhang C, Chang WC, Zhang LS, Zhang XT, Tang RH, Garg V, Wang XJ, Tang HB, Chow CN, Wang JP, Deng Y, Wang DP, Khan AW, Yang Q, Cai TC, Bajaj P, Wu KC, Guo BZ, Zhang XY, Li JJ, Liang F, Hu J, Liao BS, Liu SY, Chitikineni A, Yan HS, Zheng YX, Shan

SH, Liu QZ, Xie DY, Wang ZY, Khan SA, Ali N, Zhao CZ, Li XG, Luo ZL, Zhang SB, Zhuang RR, Peng Z, Wang SY, Mamadou G, Zhuang YH, Zhao ZF, Yu WC, Xiong FQ, Quan WP, Yuan M, Li Y, Zou HS, Xia H, Zha L, Fan JP, Yu JG, Xie WP, Yuan JQ, Chen K, Zhao SS, Chu WT, Chen YT, Sun PC, Meng FB, Zhuo T, Zhao YH, Li CJ, He GH, Zhao YL, Wang CC, Kavikishor PB, Pan RL, Paterson AH, Wang XY, Ming R, Varshney RK (2019) The genome of cultivated *peanut* provides insight into legume karyotypes, polyploid evolution and crop domestication. Nat Genet 51:865–. https://doi.org/10.1038/s41588-019-0402-2

Figures

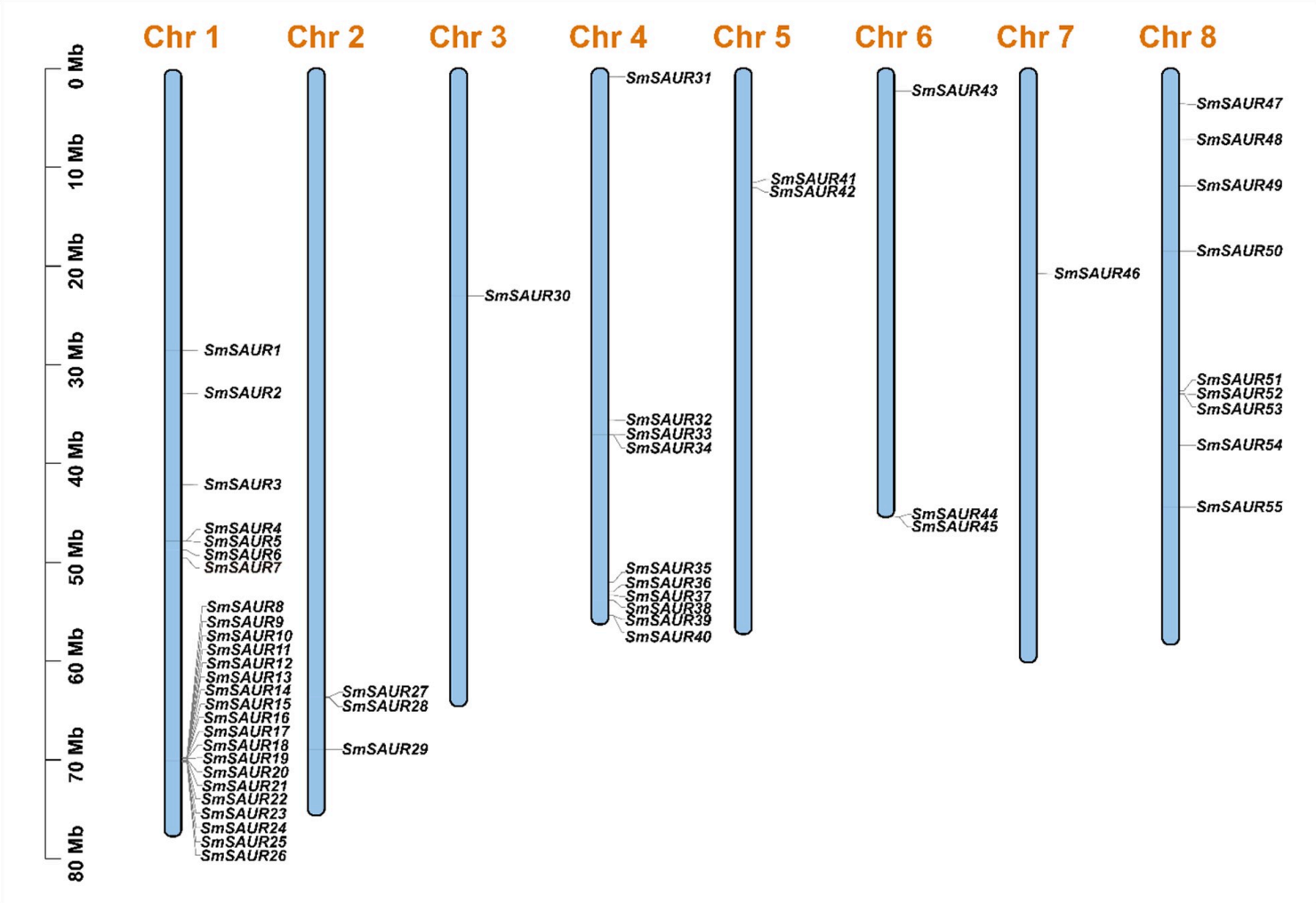


Figure 1

Chromosome mapping of the *S. miltiorrhiza SAUR* gene family. Chromosomal information for *SmSAUR*genes was obtained from the *S. miltiorrhiza* genome annotation results and mapped to the corresponding chromosomes. The scale on the left is used to estimate the chromosome lengths. The blue boxes represent the chromosomes of *S. miltiorrhiza*. The *SmSAUR* gene family members are marked in black. The chromosome number is shown on the top of each chromosome.

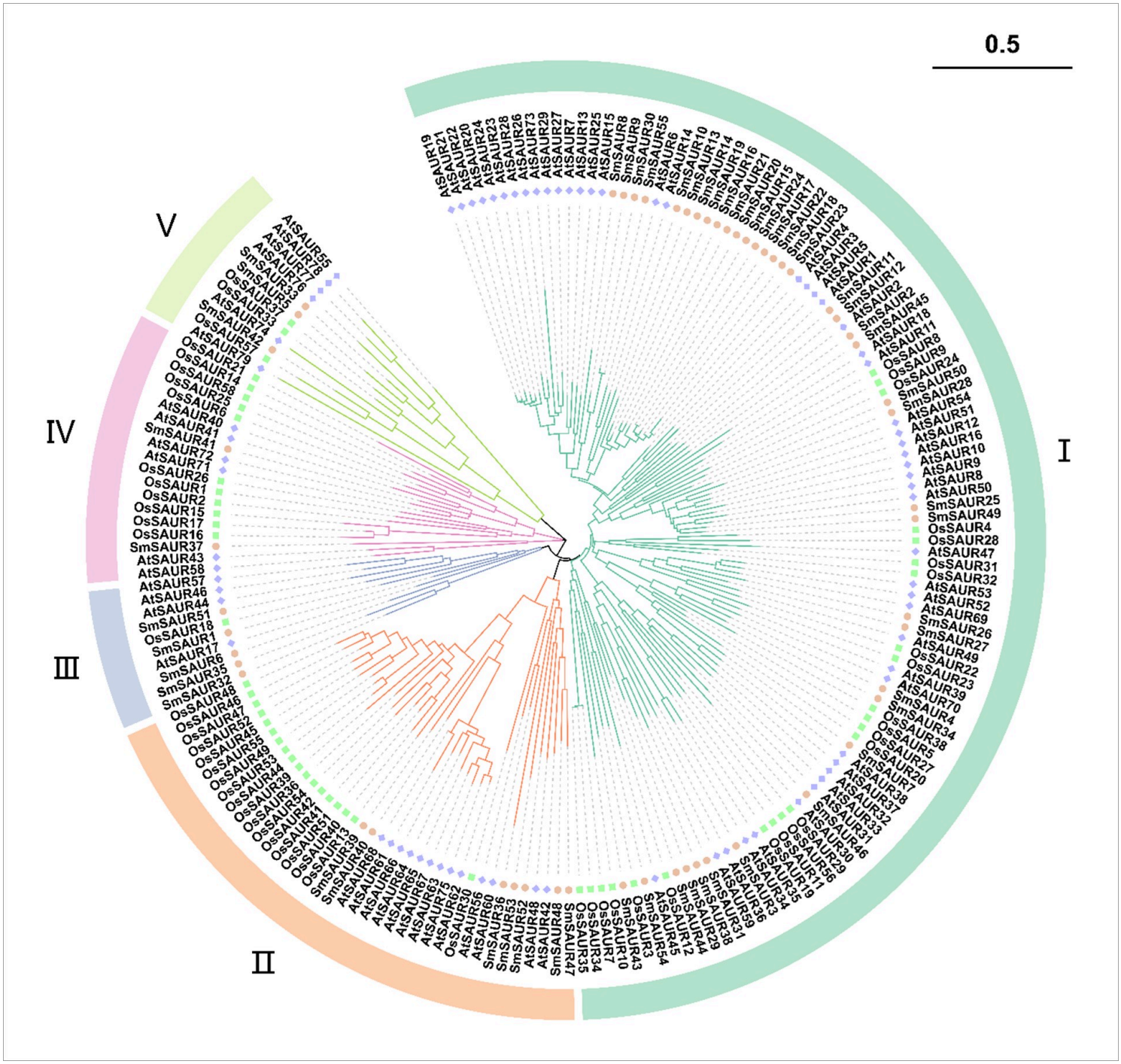


Figure 2

Phylogenetic analysis of SAURs in *S. miltiorrhiza*, *A. thaliana*, and *O. sativa*. Different *SAURs*in the three species are divided into five distinct groups, and the branches of these groups were colored differently. Different symbols outside the branches represent different species, among which orange circles, purple diamonds and green squares represent *S. miltiorrhiza*, *A. thaliana,* and *O. sativa,* respectively. Different branch lengths represent the degree of difference among the evolution of SAURs (bar = 0.5).

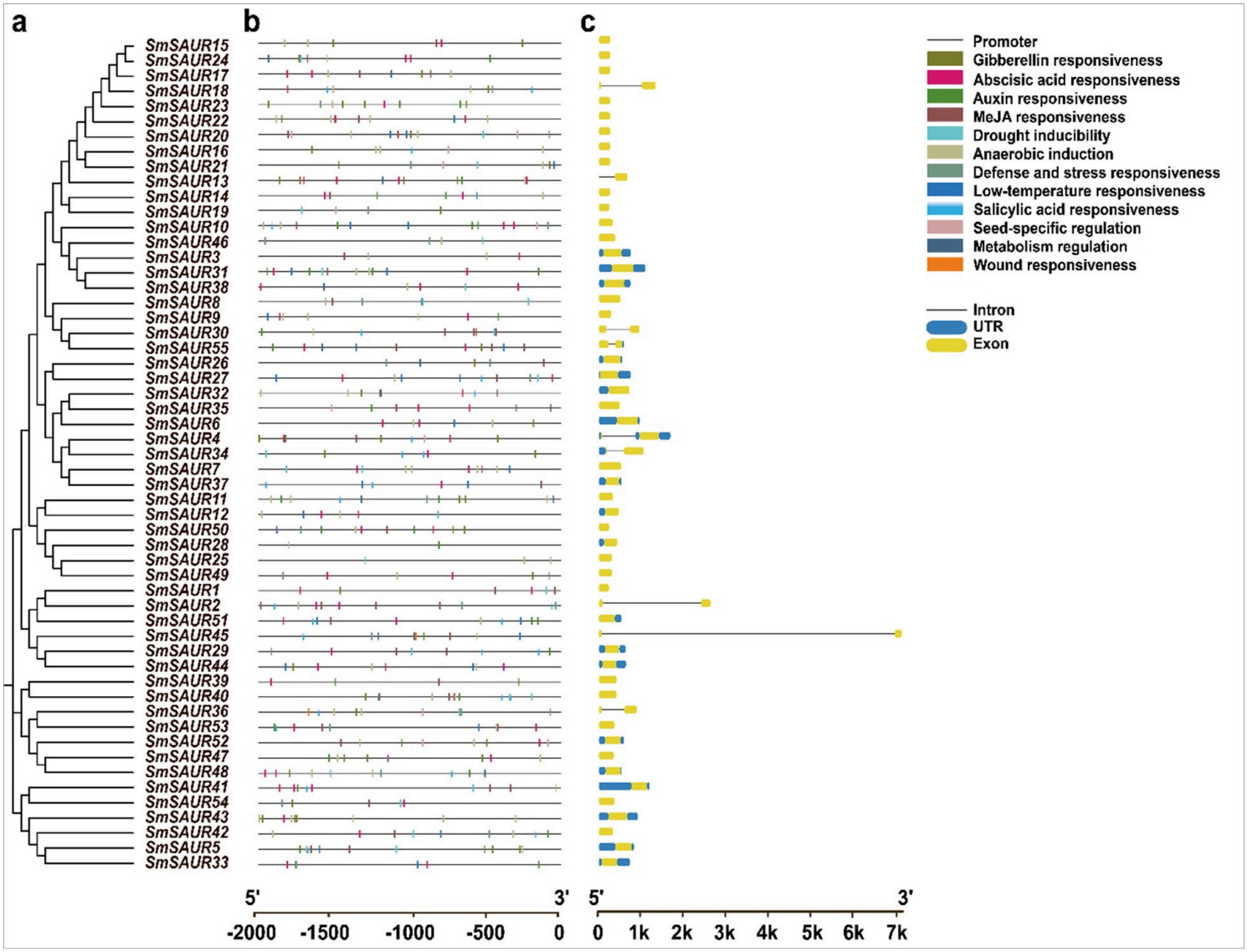


Figure 3

Phylogenetic analysis, *cis*-acting elements and gene structure of *SmSAURs* in *S. miltiorrhiza*. **a** The phylogenetic tree of SmSAUR family proteins. The phylogenetic tree was generated using the neighbor-joining (NJ) method, and a bootstrap analysis was conducted with 1000 iterations. **b** *Cis*-elements in promoters of *SmSAUR*genes. Different colored boxes represent *cis*-acting elements with different functions. **c** The gene structure of *SmSAURs*. Black lines, blue-filled boxes and yellow-filled boxes indicate introns, untranslated regions (UTRs), and Exons, respectively.

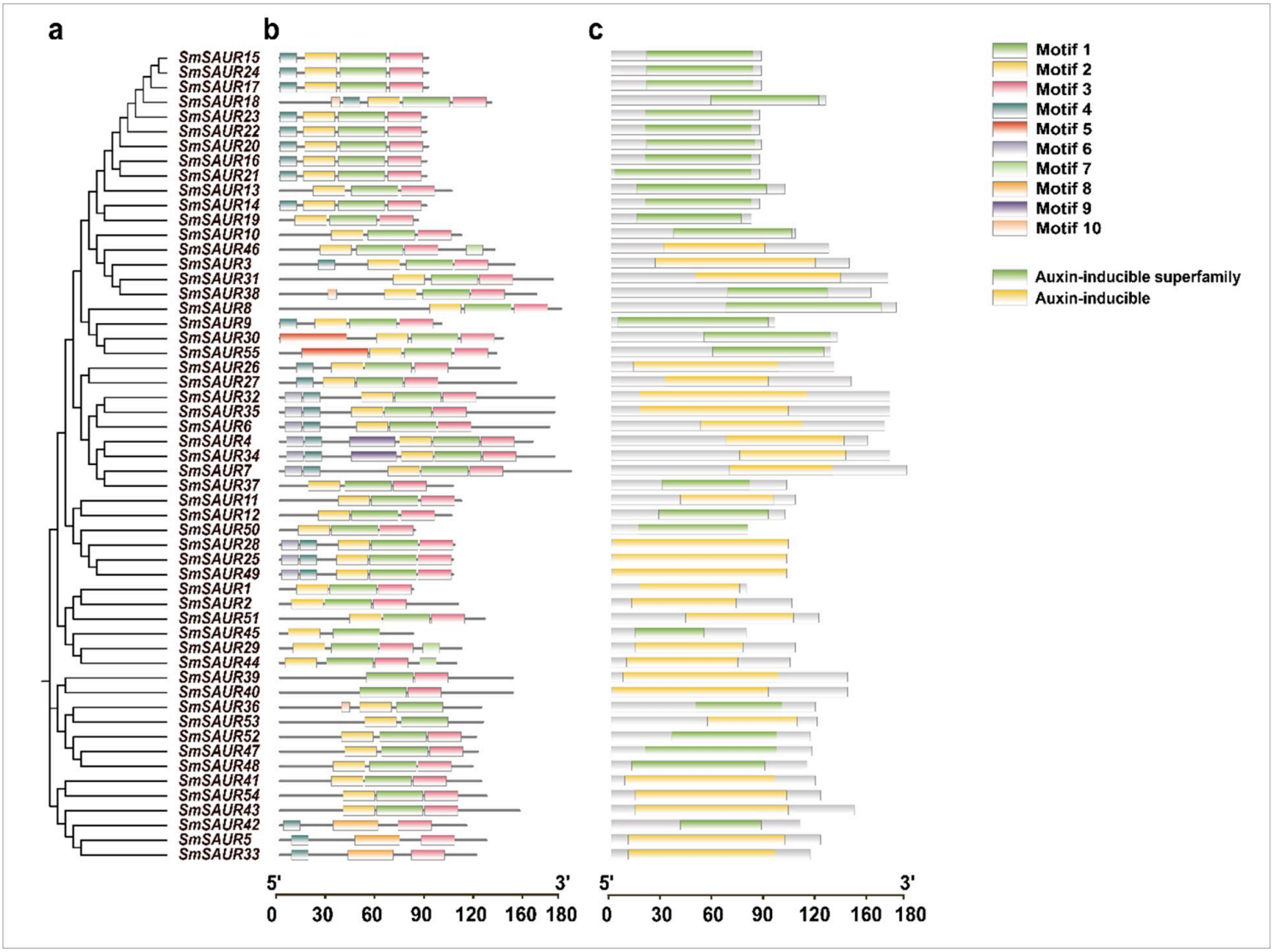


Figure 4

Phylogenetic analysis, motifs, and conserved domains of *SmSAUR* gene family in *S. miltiorrhiza* **a** The phylogenetic tree of SmSAUR proteins was constructed. **b** Conservative motif distribution of SmSAUR proteins. Different colors boxes represent different putative motifs. **c** Auxin-inducible (yellow-filled boxes) and Auxin-inducible superfamily domain (turquoise-filled boxes) of SmSAURs.

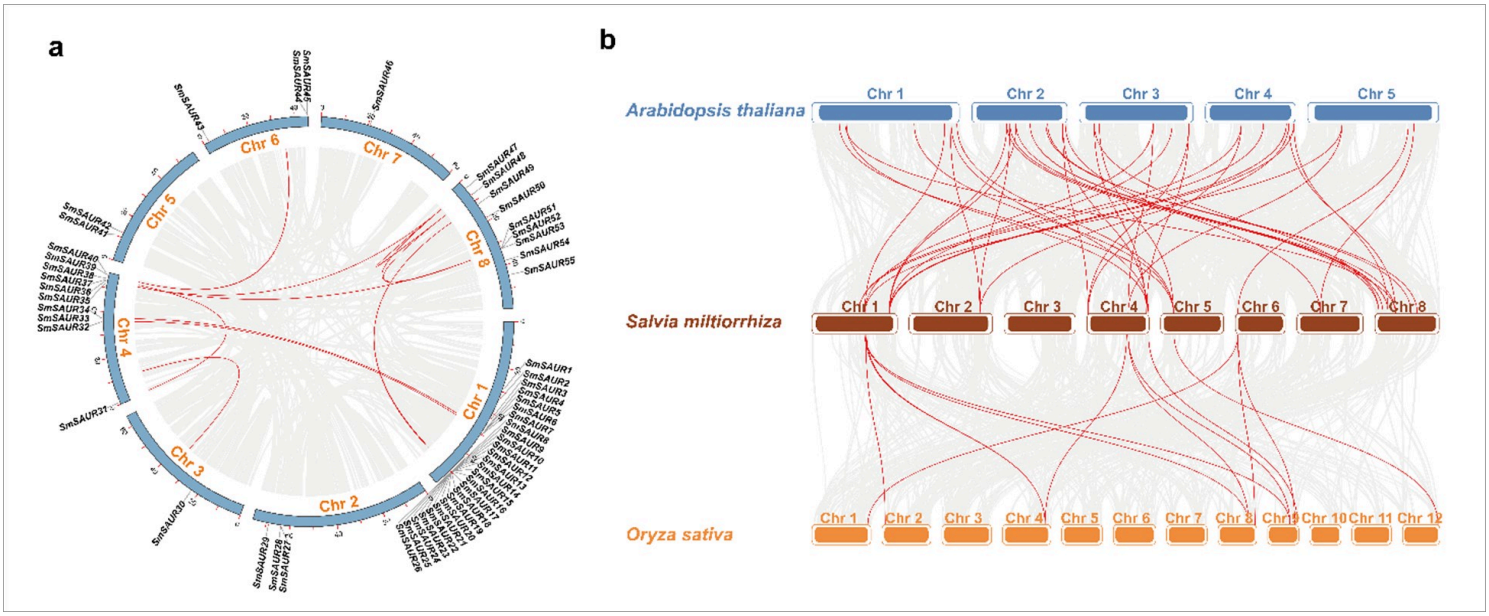


Figure 5

Synteny analysis of *SAUR* genes **a**Synteny analysis of *SmSAURs* in *S. miltiorrhiza*. The blue circles represent the 8 chromosomes of *S. miltiorrhiza*. The gray line represents all syntenic blocks in the genome of *S. miltiorrhiza*, and the red lines represent duplicate *SmSAUR* gene pairs. **b-i** Synteny analysis of *SAUR* genes among *S. miltiorrhiza, A. thaliana,* and *O. sativa*. The chromosomes of the three species are marked with different colors. Gray lines represent the collinear blocks within *S.miltiorrhiza*, *A. thaliana*, and *O. sativa*. Red lines show the orthologous relationships of *SAUR* genes among *S. miltiorrhiza*, *A.thaliana,* and *O. sativa*.

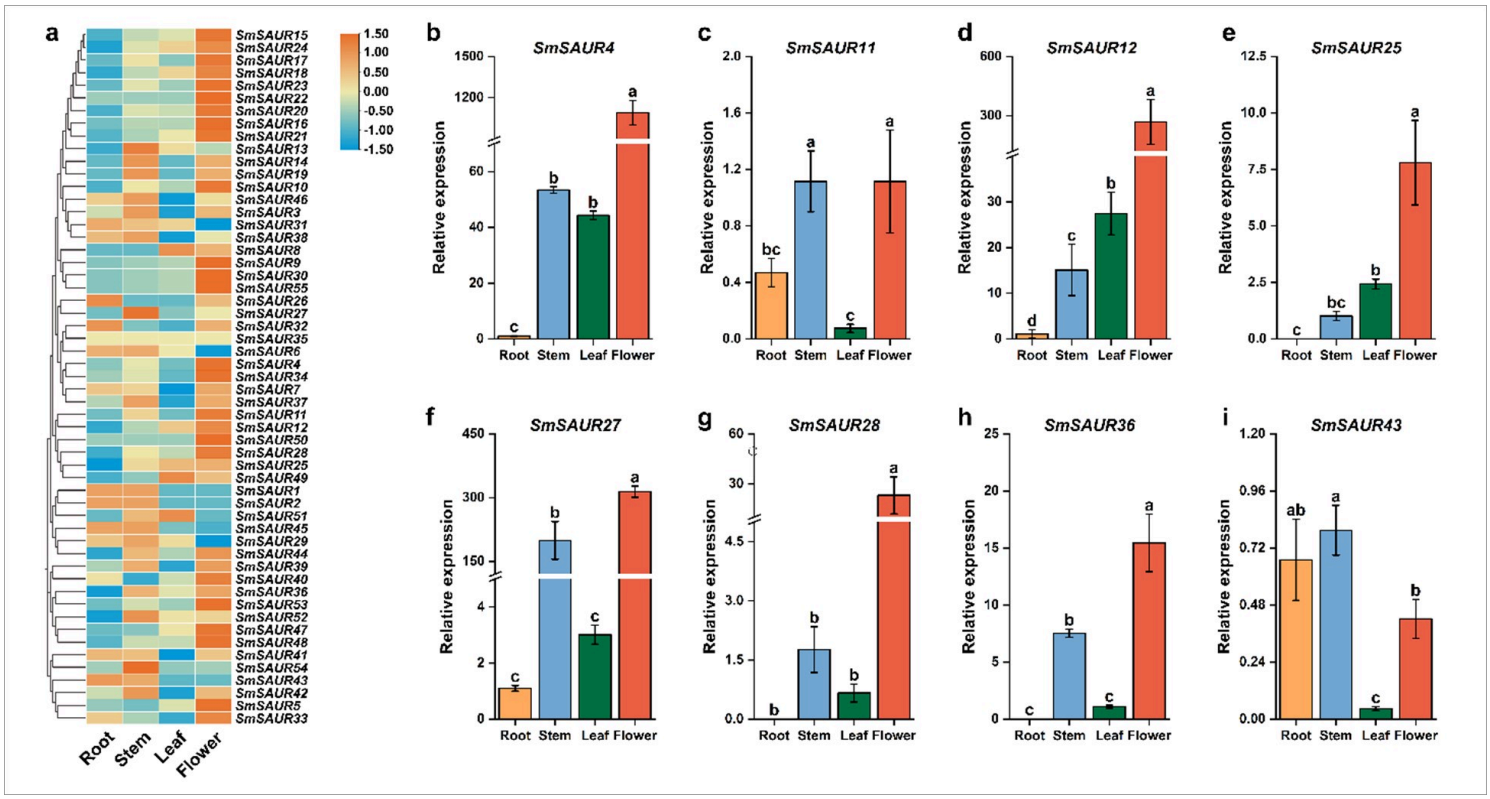


Figure 6

The expression profiles of *SmSAURs*in different organs of *S. miltiorrhiza*. **a** The heatmap depicting the expression profiles of *SmSAURs* in different organs. Changes in expression levels are represented with different colors, the orange indicates a higher expression level, and the blue indicates a lower expression level. **b** The qRT-PCR validations of relative expression levels of eight randomly selected genes from *SmSAUR* gene family. The error bars represent means ± SD (n= 3). Different lowercase letters on the bar chart indicate differences in significance tested following Duncan's one-way multiple-range post hoc ANOVA (P< 0.05).

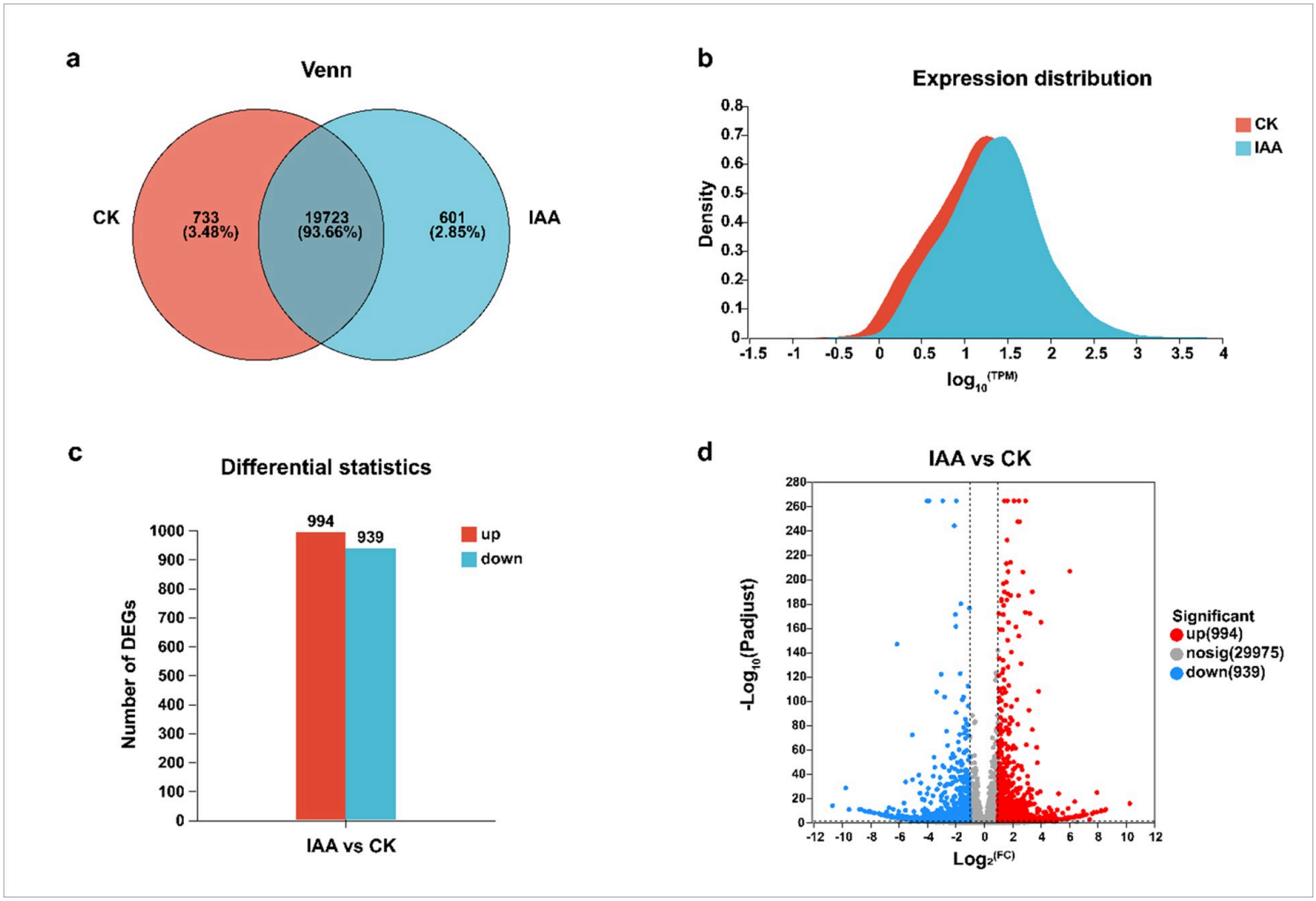


Figure 7

RNA-seq analysis of the IAA-treated and control groups in *S. miltiorrhiza*. **a** The Venn diagram of DEGs in the two groups. **b** Expression distribution of genes based on TPM values. **c** Number of DEGs in the two groups (control and IAA). **d** Volcano plot of the DEGs with the cutoff ($|\log_2^{(\text{Fold change})}| \geq 1$ and FDR < 0.05) in the two groups. The red color represents up-regulated DEGs, the blue color represents down-regulated DEGs, and the gray color represents the non-DEGs. CK, the control group; IAA, the IAA-treated group.

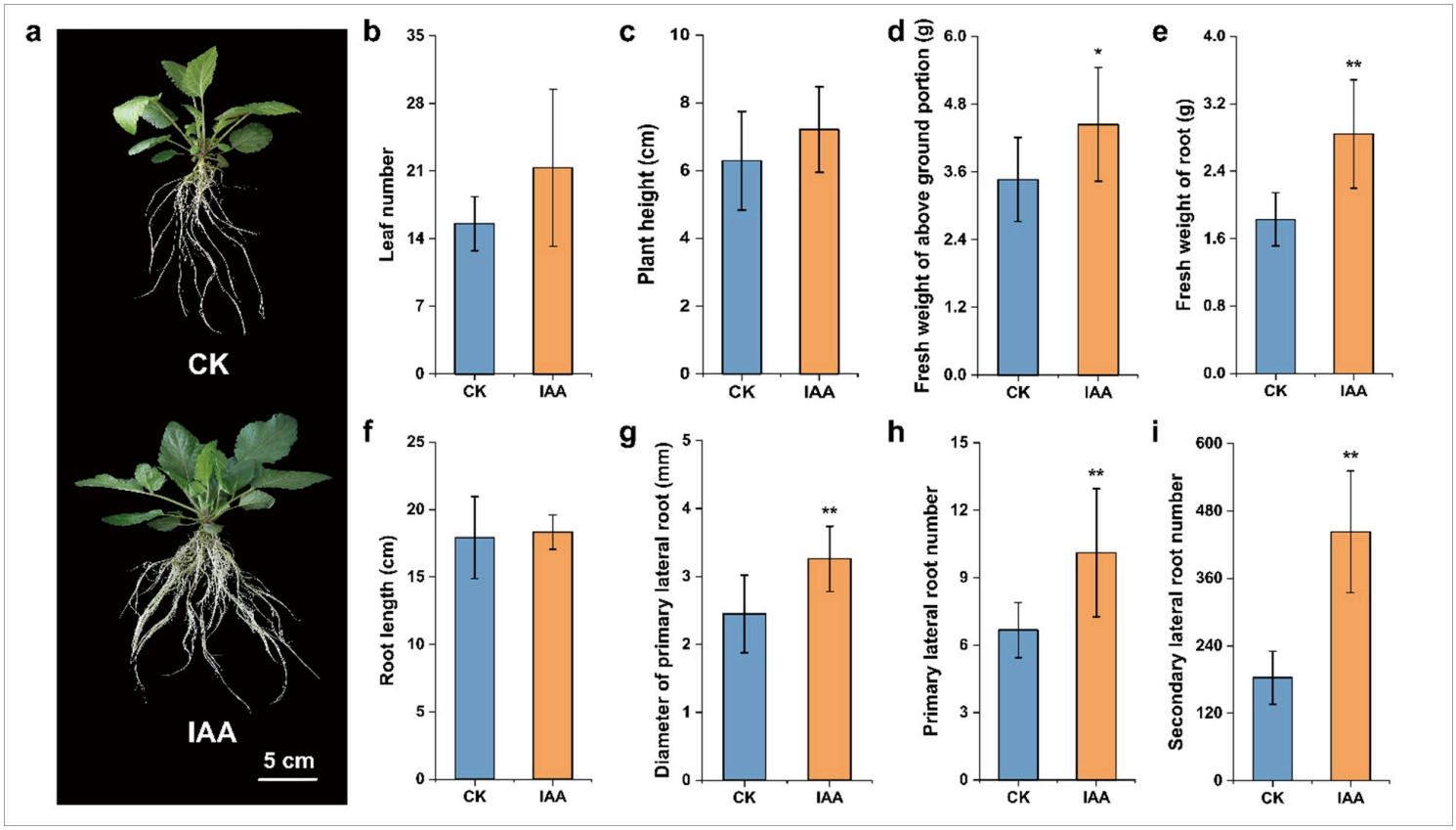


Figure 8

Effects of exogenous IAA application on growth and lateral root development of *S. miltiorrhiza*. **a** Phenotype of *S. miltiorrhiza* seedlings in the IAA-treated and control groups. **b-d** The growth indexes in the different groups. **e-i** The root morphological indexes in the different groups. CK, the control group; IAA, the IAA-treated group. The error bars represent means ± SD (n = 3). Statistically significant differences between different treated groups are calculated based on the paired-sample t-tests: * P < 0.05; ** P< 0.01.

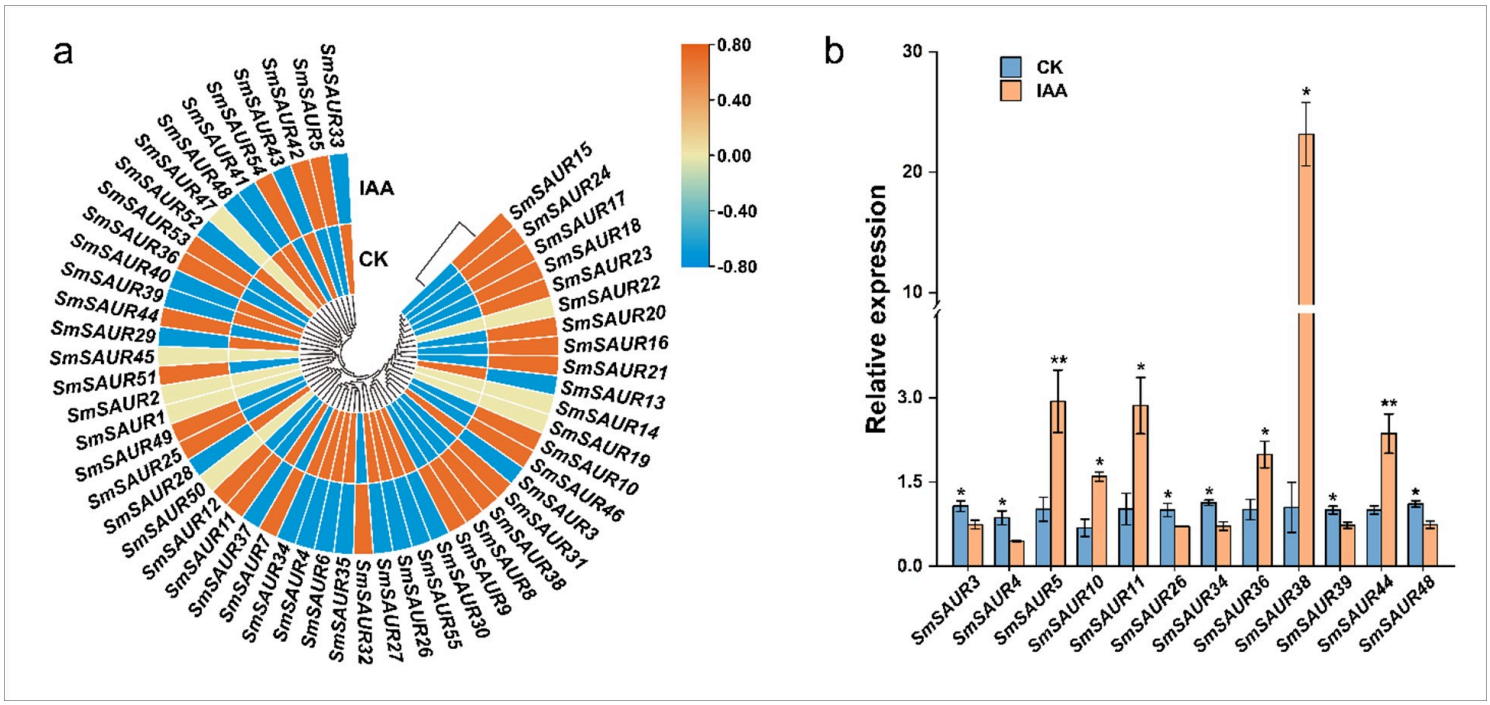


Figure 9

Expression patterns of *SmSAURs* in the IAA-treated and control groups in *S. miltiorrhiza*. **a** The heatmap depicting the expression profiles of *SmSAURs*. The expression levels in different groups are represented with different colors. The orange color indicates a higher expression level, and the blue color

indicates a lower expression level. **b** The qRT-PCR validations of relative expression levels of twelve randomly selected genes from *SmSAUR* gene family. CK, the control group; IAA, the IAA-treated group. Different treated groups are shown by different colors. These data are normalized relative to the internal control *SmActin* and is shown as the means ± SD of three independent biological repetitions. Statistically significant differences between different treated groups are calculated based on the Student's t-tests: * $P < 0.05$; ** $P < 0.01$.

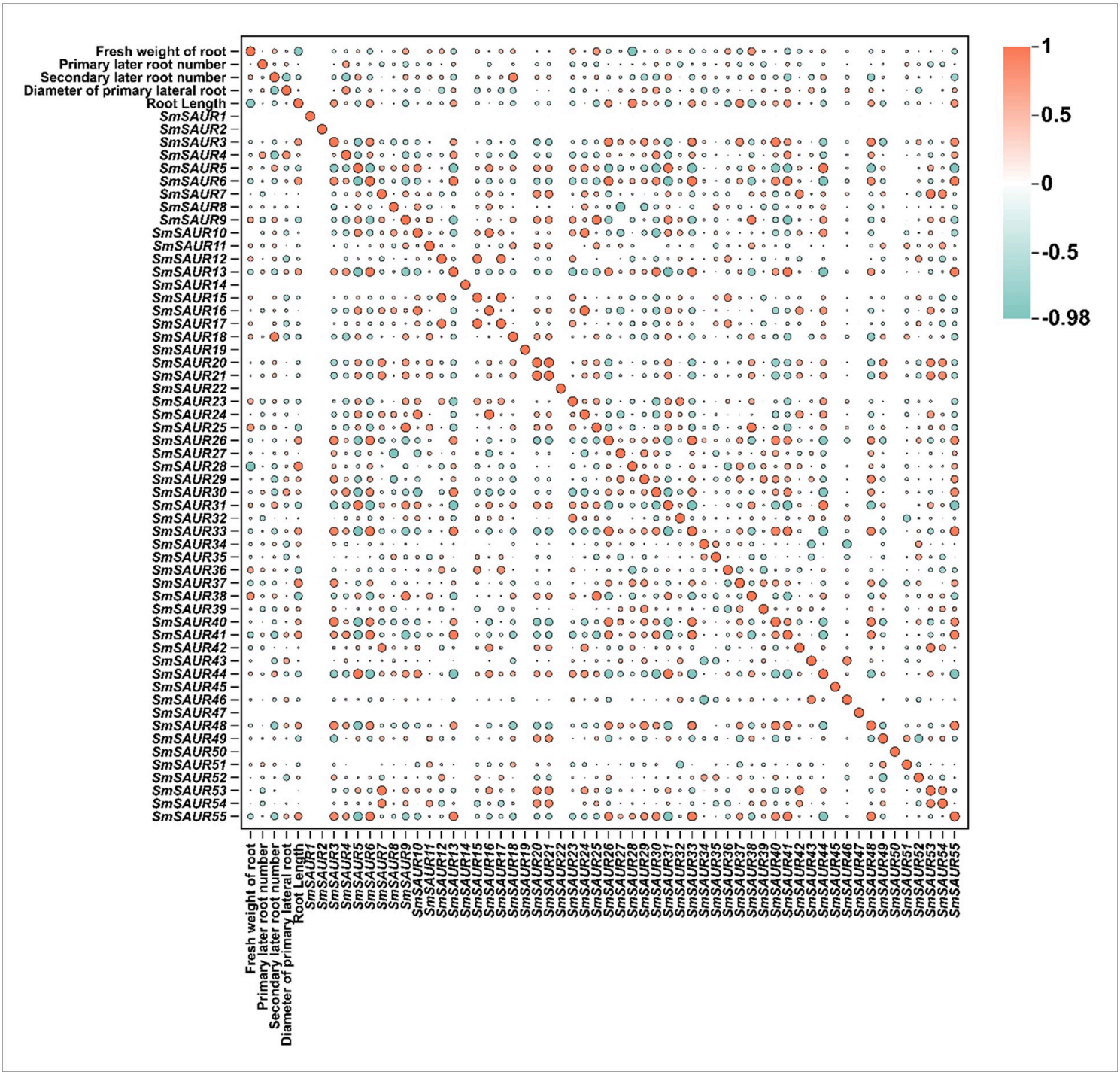


Figure 10

Pearson correlation coefficient analysis to screen the potential *SmSAUR* genes being involved in root development in *S. miltiorrhiza*. The size of the circles represents the degree of association between the *SmSAUR* genes and root development; green circles represent a negative correlation, while orange circles represent a positive correlation. The absence of a circle indicates no correlation.

Supplementary Files

This is a list of supplementary files associated with this preprint. Click to download.

- TableS1.xls

- TableS2.xls
- TableS3.xls
- TableS4.xls
- TableS5.xls
- TableS6.xls
- TableS7.xls
- TableS8.xls
- floatimage11.jpg